

Exploring Algal Tocopherol for Antioxidant Applications

M.Sc. Thesis

By

MAHESH SAHU



**DEPARTMENT OF BIOSCIENCES AND BIOMEDICAL
ENGINEERING
INDIAN INSTITUTE OF TECHNOLOGY INDORE
MAY 2025**

Exploring Algal Tocopherol for Antioxidant Applications

A THESIS

*Submitted in partial fulfillment of the
requirements for the award of the degree
of*
Master of Science

By
MAHESH SAHU



**DEPARTMENT OF BIOSCIENCES AND BIOMEDICAL
ENGINEERING
INDIAN INSTITUTE OF TECHNOLOGY INDORE
MAY 2025**

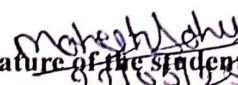


INDIAN INSTITUTE OF TECHNOLOGY INDORE

CANDIDATE'S DECLARATION

I hereby certify that the work which is being presented in the thesis entitled **EXPLORING ALGAL TOCOPHEROL FOR ANTIOXIDANT APPLICATIONS** in the partial fulfillment of the requirements for the award of the degree of **MASTER OF SCIENCE** and submitted in the **DEPARTMENT OF BIOSCIENCES AND BIOMEDICAL ENGINEERING, INDIAN INSTITUTE OF TECHNOLOGY INDORE**, is an authentic record of my own work carried out during the time period from August 2023 to May 2025 under the supervision of Prof. Kiran Bala, Department of Biosciences and Biomedical Engineering, Indian Institute of Technology Indore.

The matter presented in this thesis has not been submitted by me for the award of any other degree of this or any other institute.


Signature of the student with date
(Mahesh Sahu)

This is to certify that the above statement made by the candidate is correct to the best of my/our knowledge.


22/5/25

Signature of the Supervisor of
M.Sc. thesis (with date)
(Prof. Kiran Bala)

Mahesh Sahu has successfully given his M.Sc. Oral Examination held on MAY 7, 2025.



Signature(s) of Supervisor(s) of MSc thesis
Date:



Convener, DPGC
Date: 23-05-2025

ACKNOWLEDGEMENTS

I would like to express my gratitude to all those who helped me throughout my journey to complete this thesis. First of all, I wish to manifest my wholehearted thanks and profound gratitude to my thesis supervisor **Prof. Kiran Bala** for providing me with opportunity to work in her lab and under whose guidance I could accomplish my M.Sc. project work.

I would express special thanks to our HOD BSBE Dr. Parimal Kar, DPGC Prof. Prashant Kodgire and all the faculty members of BSBE for their kind support, encouragement and inspiration. I am highly grateful to all my AETS lab members, seniors, juniors and classmates for all their time and efforts provided to me in my journey making me to learn many new things, grow more during the execution of my project work and providing me with a family away from home. I pay my devoted thanks to my lab seniors Ms. Rimjhim Sangtani, who consistently guided and motivated me at each step of my project work. I am also really thankful to Ms. Anshul Kaushik, Ms. Konika Katare, Ms. Kanika Kiran, Dr. Palak Saket, Mr. Dinesh Parida, Dr. Bikash Kumar, for continuous care, cheer, and guidance throughout the project that has been a source of inspiration for me to complete my thesis. I am also thankful to my lab colleagues Ms. Neha, Ms. Namita, Ms. Yogita and Ms. Rishika for continuous motivation and help. I am also thankful to field emission scanning electron microscope (FE-SEM) facility equipped at Sophisticated Instrument Centre (SIC), IIT Indore. I am highly grateful to our department BSBE, IIT Indore for providing us with such an excellent research platform making our works smoother and better. I would also like to acknowledge all of my family and friends for their kind support during this journey. Above all, my heartfelt thanks to Almighty God for granting me the strength throughout the journey and everyone else who directly or indirectly helped me.

*Dedicated to my family, lab
seniors and my friends*

Abstract

Oxidative stress, often resulting from the massive production of ROS (reactive oxygen species), has been a significant reason behind cell damage, cell maturation, and the commencement of chronic diseases like neurological complications, cardiovascular problems, and cancer. The human body's defense mechanism consists of endogenous antioxidants; however, recent environmental or pathological conditions have made these mechanisms inefficient, thus demanding the uptake of exogenous antioxidants. Amidst the availability of various broad-spectrum naturally extracted antioxidants, tocopherol, part of the vitamin E family, has been identified widely for its capability of effectively scavenging free radicals, inhibiting lipid peroxidation, and complete protection of cells. Typically, plant resources like sunflowers, soybean seeds, etc., have been utilized to extract tocopherol. However, the extreme dependency on agricultural crops and land, very low yield, differences in the tocopherol yield due to seasonal variability, and complicated extraction protocol limit the upscaling and industrial applications of tocopherol extracted from plant sources.

In the past few years, microalgae have become an attractive substitute for sustainably producing high-value-added bioactive metabolites, like polyunsaturated fatty acids, tocopherols, pigments, etc. Microalgae have numerous benefits, such as rapid cell growth, highly versatile biochemical profile, and survival ability in extreme environmental conditions, positioning them as a strong contender for large scale production of antioxidant in industrial applications. Essentially, certain algal strains have been reported to have a significant quantity of tocopherols. However, the increase in the tocopherol yield has been recorded in response to certain abiotic stress factors, thus making microalgae an ideal model microorganism to elucidate the stress-induced metabolite

enrichment. Even though microalgae have immense potential, very few studies evaluate the tocopherol production potential of different microalgal species under such varying environmental perturbations.

Therefore, the current study has been designed to understand and compare the tocopherol yield of six different native microalgal strains: IMMA 11, IMMA 12, IMMA 13, IMMA 14, IMMA 15, and IMMA 16. The investigation was framed in two stages, i.e., screening of algal species followed by optimizing abiotic stress conditions for tocopherol yield. Primarily, cell kinetics, biomass, chlorophyll accumulation, and tocopherol yield of all six species were assessed at different growth phases, such as 7th, 14th, 21st, and 28th Day. IMMA 12 exhibited the highest biomass accumulation and growth of all these species but relatively lower tocopherol, whereas IMMA 14 showed the highest yield despite the minimal biomass accumulation and growth.

On the basis of the findings of the screening, both IMMA 12 and IMMA 14 were selected for further investigation under abiotic stress parameters, such as varying light intensities (3000, 9000, 15000 Lux), photoperiod/light: dark period (12:12, 16:8, and 24:0), and sodium chloride concentrations (0, 50, 150, 250 mM). The results revealed that IMMA 14 outperformed IMMA 12 in α -tocopherol content by 144.64 %. Further, microscopy of selected samples also revealed the morphological changes under stress. The crude extract containing the highest tocopherol also exhibited hydrogen peroxide scavenging activity. In a nutshell, the current research highlights the diverse stress response of different microalgal strains for the biosynthesis of tocopherol and reinforces that microalgae is a potential antioxidant source for nutraceutical applications.

LIST OF PUBLICATIONS

- Sahu, M., Sangtani, R., Kaushik, A., Bala, K., “Exploring the antioxidant molecule from native algal species for nutraceutical applications”. (*manuscript under preparation*)

TABLE OF CONTENTS

List of Figures	XV
List of Tables	XVII
Abbreviations	XIX
Chapter 1: Introduction	
1.1. Oxidative stress and its role in disease pathophysiology	1-7
1.2. Algae and its significance	
1.3. Organization of the thesis	
Chapter 2: Literature review	
2.1. Antioxidants	
2.2. Algal metabolites as antioxidants	8-20
2.3. Biochemical classification of algal isoprenoid lipids with emphasis on tocopherols	
2.4. Factors affecting algal tocopherol production	
Chapter 3: Hypothesis and objectives	
3.1. Hypothesis	21-23
3.2. Objectives of the study	
Chapter 4: Materials and methodology	24-41

4.1. Materials

4.2. Methodology

4.3. Workplan

Chapter 5: Results and Discussion

5.1. Characterisation of native microalgal species

5.2. Experiment on selected microalgal species IMMA 12 42-59

5.3. Experiment on selected microalgal species IMMA 14

5.4. Estimating in-vitro hydrogen peroxide scavenging
activity α -tocopherol rich extract

Chapter 6: Conclusions and future perspectives

6.1. Conclusions 60-62

6.2. Future perspectives

References 63-72

LIST OF FIGURES

Figure 1. Illustration of oxidative stress in CVD (adapted from Mourino-Alvarez et al., 2022)

Figure 2. Algae and its major types (Thoré et al., 2023)

Figure 3. Mechanism of secondary metabolites production

Figure 4. Isoprenoids classification

Figure 5. Mechanism of ROS production and destruction (Udaypal et al., 2024)

Figure 6. Diagrammatic representation of hypothesis

Figure 7. (A, B, C, D, E, F) shows the relation between OD and dry weight of the six microalgal species under study.

Figure 8. Prominence-i, LC-2030C 3D PLUS HPLC equipped with a fluorescence detector (RF-20A) CIF, BSBE, IIT Indore)

Figure 9. Chromatogram A) α -tocopherol standard peak (10 ppm); B) Microalgal α -tocopherol rich extract peak

Figure 10. Experimental work plan with algal species for morphological, growth and biochemical characterization

Figure 11. Experimental flasks of microalgae, IMMA 12 under abiotic factor conditions in the BG 11 media

Figure 12. Diagrammatic representation of combination of abiotic factors in experimental flasks of IMMA 12

Figure 13. Experimental work plan with algal species for morphological, growth and biochemical characterization

Figure 14. Diagrammatic representation of combination of abiotic factors in experimental flasks of IMMA 14

Figure 15. Depicting the different morphology shape and size of native microalgal species (A) IMMA 11, (B) IMMA 12, (C) IMMA 13, (D) IMMA 14, (E) IMMA 15, (F) IMMA 16

Figure 16. The growth curve depicting the growth characteristic of 6 native microalgal species

Figure 17. The graph depicts the biomass accumulation of the 6 different native microalgal species at 5 different time point

Figure 18. Graph depicting the chlorophyll profile of microalgal species at 4 different days of different growth phase

Figure 19. Tocopherol standard calibration curve

Figure 20. The graph depicts the tocopherol content in 6 native microalgal species (IMMA 11- IMMA 16) measured over 4 time points in different growth phase.

Figure 21. Biomass accumulation and chlorophyll content under 27 different abiotic factor combinations (A) 3000 Lux; (B) 9000 Lux; (C) 15000 Lux

Figure 22. α -TE accumulation in IMMA 12 under 27 different abiotic factor combinations (A) 3000 Lux; (B) 9000 Lux; (C) 15000 Lux

Figure 23. SEM images of IMMA 12 species of Microalgae at lowest and highest abiotic factor

Figure 24. Biomass and chlorophyll accumulation of IMMA 14 under 18 different abiotic factor combinations (A) 3000 Lux; (B) 9000 Lux; (C) 15000 Lux

Figure 25. α -TE accumulation in IMMA 14 under 18 different abiotic factor combinations (A) 3000 Lux; (B) 9000 Lux; (C) 15000 Lux

Figure 26. SEM characterization of IMMA 14 under (A) Control ($L_3P_{12}S_{50}$) (B) $L_9P_{12}S_{50}$ (C) Highest stress ($L_{15}P_{24}S_{150}$)

LIST OF TABLES

Table 1. Tocopherol yield of different food groups

Table 2. Factors affecting algal tocopherol production

Table 3. Composition of BG-11 media

Table 4. Microalgal growth kinetics at log phase

Table 5. Antioxidant activity assay of α -tocopherol rich algal extract

ABBREVIATIONS

BG-11- Blue green -11

CHL-Chlorophyll

OD- Optical density

α -TE- α -tocopherol

P- Biomass productivity

DW- Dry weight

MeOH -Methanol

ACN- Acetonitrile

ROS- Reactive oxygen species

RNS- Reactive nitrogen species

OS- Oxidative stress

UV- Ultra-violet

PUFA- Polyunsaturated fatty acids

CVD- Cardio-vascular diseases

CKD- Chronic-kidney disease

COPD- chronic obstructive pulmonary disease

LDL- Low-density lipoprotein

SEM- Scanning electron microscope

HPLC- High-performance liquid chromatography

Chapter 1

Introduction

Helmut Sies first gave the term ‘oxidative stress’ (Jones & Radi, 2014). Oxidative stress is a harmful biological condition mainly caused by the disturbance of equilibrium between the production and removal of reactive oxygen species (ROS), reactive nitrogen species (RNS), and various other free radicals that are found within cells and tissues. This unbalanced condition causes potential damage to cellular components and other biomolecules such as DNA, lipids, and proteins. ROS are generally generated as a by-product of oxygen metabolism in organelles like mitochondria and various environmental stressors (such as UV, ionizing radiation, pollutants, and xenobiotics) (Pizzino et al., 2017). Mitochondria is the cell's energy center; it utilizes oxygen for energy production and produces ROS that results in oxidative stress and damages the cell structure, lipids, protein, and DNA. Oxidative stress is implicated in many diseases where the alteration of mitochondrial proteins, DNA, and lipids leads to the damage of nerve cells and other metabolically active cells (Sawhney, 2019).

Reactive oxygen species (ROS) comprise both free radicals like hydroxyl radicals (OH^\cdot) and superoxide anions (O_2^-), as well as non-radical compounds such as hydrogen peroxide (H_2O_2). These are regarded as pro-oxidant molecules that promote the oxidation of biomolecules. It has a dual function in both normal physiological processes and the development of diseases. These free radical and ROS cause the progression of many diseases, such as diabetes, diabetic neuropathy, nephropathy, obesity, and neurological diseases like Alzheimer's and Parkinson's. It is also one reason for the onset of cardiovascular, inflammation, and cancer (Reddy, 2023). Generally, ROS is considered harmful to the human body and has deleterious effects.

However, this is not entirely true; ROS are involved in physiological signaling, gene expression, various enzyme activities, and defense mechanisms. However, their overproduction or an insufficient antioxidant response result in the progression of oxidative stress (Voronkova et al., 2018; Yamasaki et al., 2025).

1.1. Oxidative stress and its role in disease pathophysiology

Oxidative stress contributes to the onset and progression of numerous diseases across multiple organs of the human body. Metabolic diseases like diabetes mellitus and obesity are one such diseases. Oxidative stress arises due to the overproduction of ROS by various mediums, such as hyperglycemia, insulin resistance, and lipid peroxidation (Onaca et al., 2010). Diabetes is characterized by elevated blood glucose levels (hyperglycemia), which promote the production of ROS, leading to oxidative stress. This disturbance between the body's antioxidant defenses and the excess ROS is a key factor in the causation and progression of diabetes and other metabolic disorders. When blood sugar levels are too high, oxidative stress occurs, causing damage to proteins, fats, and DNA. This damage affects cell membrane, essential cellular processes, including insulin signaling and the function of insulin-producing β -cells. ROS are mainly generated in parts of the cell, like the phagocytic cells, mitochondria, endoplasmic reticulum, and peroxisomes, with the mitochondrial electron transport chain serves as a primary contributor. To reduce the harmful effects of ROS, the body uses its natural antioxidants or relies on external ones to maintain balance and protect cells. If left unchecked, excessive ROS can lead to complications in small and large blood vessels, worsening the effects of diabetes (Bhatti et al., 2022).

Likewise, as shown in **Figure 1**, cardiovascular diseases (CVD) are another disease revolving around oxidative stress. CVD is a global health

challenge. Excess ROS in vascular cells leads to endothelial dysfunction, oxidation of low-density lipoprotein (LDL), and activation of pro-inflammatory pathways, promoting atherosclerosis, hypertension, ischemic heart disease, heart failure, and cardiac arrhythmia. Oxidative stress-induced dysregulation of vasoactive factors and enzymes such as NADPH oxidase and xanthine oxidase exacerbates vascular injury (admins, 2024). Increased lipid peroxidase and reduced antioxidant molecules in plasma are pfurther proportional to the severity of the disease (Katoch et al., 2013).

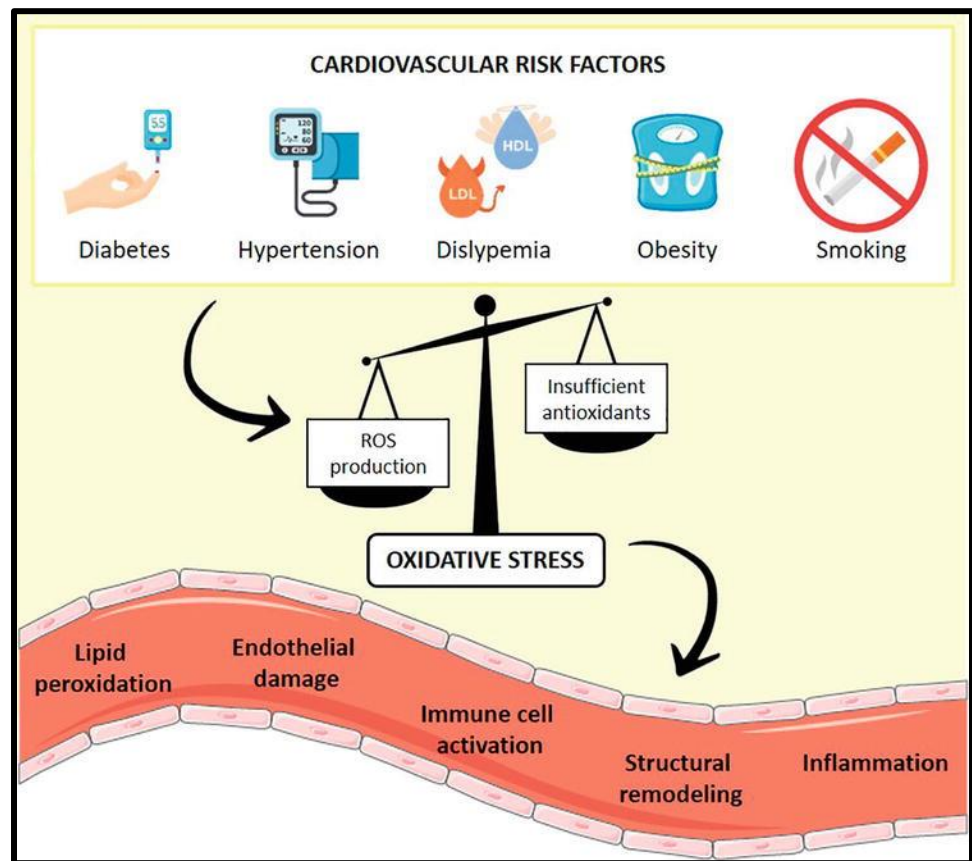


Figure 1. Illustration of oxidative stress in CVD (adapted from (Sastre-Oliva et al., 2022)).

Neurodegenerative diseases also involve oxidative stress. Aging of cells increases oxidative stress, and mitochondrial dysfunction is elevated in neurodegenerative diseases such as Parkinson's, Alzheimer's,

Huntington's, and prion diseases (Casetta et al., 2005). ROS-associated damage to neuronal DNA, lipids, and proteins leads to neuronal death via apoptosis or necrosis. Free radical production in excess leads to loss of neurons, which further causes dementia. Antioxidant therapies show promise in experimental models, but their clinical effectiveness has remained limited (Casetta et al., 2005).

Chronic kidney disease (CKD) has been a major health problem in humans worldwide, mostly in developed countries. Oxidative stress in CKD arises from reduced renal function and systemic inflammation due to comorbidities like diabetic nephropathy and hypertension and treatment like hemodialysis, contributing to cardiovascular complications and renal injury progression (Modaresi et al., 2015). Oxidative stress also retards the renal blood flow by vasoconstricting the vascular smooth muscle cell (Dobrek, 2022). Similarly, pulmonary & respiratory diseases are also related to oxidative stress. Exogenous sources of ROS, like cigarette smoking, environmental pollutants as well as endogenous inflammatory responses, cause oxidative injury in the respiratory system, which leads to various respiratory diseases, including asthma, chronic obstructive pulmonary disease (COPD), acute lung injury, and rare respiratory disorders (Boukhenouna et al., 2018; Menzel et al., 2019). Oxidative stress exacerbates airway inflammation, impairs antiviral responses, and damages epithelial barriers

Autoimmune diseases including rheumatoid arthritis and multiple sclerosis also show enhanced oxidative stress, leading to increased inflammation, apoptosis, and breakdown of self-tolerance (Kumagai et al., 2003). Cancer cells also produce elevated ROS, which participates in DNA mutations, cell proliferation, and resistance to apoptosis. Although high ROS levels are known to be detrimental, moderate levels lead to tumor progression and survival, presenting a dual role (Andonova et al., 2015). Further oxidative stress is also known to be associated with reproductive

health and fertility. Oxidative stress affects both male and female reproductive systems by damaging sperm DNA, impairing sperm motility, causing oocyte quality decline, and disrupting hormonal balance (Wang et al., 2025; Wróblewski et al., 2024). This contributes to infertility and poor reproductive outcomes. Female reproductive disorders and complications such as polycystic ovary syndrome, endometriosis, and recurrent pregnancy loss have been linked to oxidative damage (Baboo et al., 2019). Assisted reproductive technologies are also affected by oxidative stress, contributing to gamete dysfunction and low success rates (Gupta et al., 2010). In gastrointestinal diseases like gastric mucosal injury, chronic pancreatitis, inflammatory bowel diseases, and gastrointestinal ulcers, ROS-induced oxidative stress is involved. Neutrophil-derived ROS and oxidative damage to DNA and lipids exacerbate inflammation, impeding healing and promoting carcinogenesis (Naito & Yoshikawa, 2011).

Antioxidant therapies aim to restore redox homeostasis by neutralizing ROS, enhancing endogenous defenses, or modulating signaling pathways involved in oxidative stress responses. They include enzymatic antioxidant mimetics (e.g., MnSOD mimetics) (Forman & Zhang, 2021), natural antioxidants (vitamins C and E, flavonoids, carotenoids, polyphenols), and synthetic molecules (Grujicic & Allen, 2024). Several natural compounds from plants, seaweeds, and amphibian peptides demonstrate antioxidative and therapeutic potential against oxidative stress-related diseases (Pradhan et al., 2021; Silva Ortíz et al., 2025). Clinical trials of antioxidant supplementation show promise but have yielded mixed results, influenced by factors such as dosing, bioavailability, and disease heterogeneity. For example, vitamin C and E supplementation reduced oxidative stress in patients with cardiovascular and Crohn's disease (Aghdassi et al., 2003). Antioxidant compounds are also being explored in neurodegenerative diseases, with some preclinical successes but facing challenges in clinical translation (Gelain et al., 2012). Emerging therapies target key antioxidant regulatory pathways, such as the Nrf2-Keap1 system

that governs cellular antioxidant gene expression. Strategies using nanomaterials, gene therapy, and redox-active molecules are still under development (Gambhir et al., 2022).

1.2. Algae and its significance

Algae are photosynthetic microorganisms that produce oxygen and utilize CO₂ and sunlight for their growth and generate an array of primary and secondary bioactive compounds, including sterols, polyphenols, carotenoids, flavonoids, phycobiliproteins, alkaloids, astaxanthin, PUFA, such as DHA and EPA, as well as polysaccharides such as β -glucan (Borowitzka, 1992).

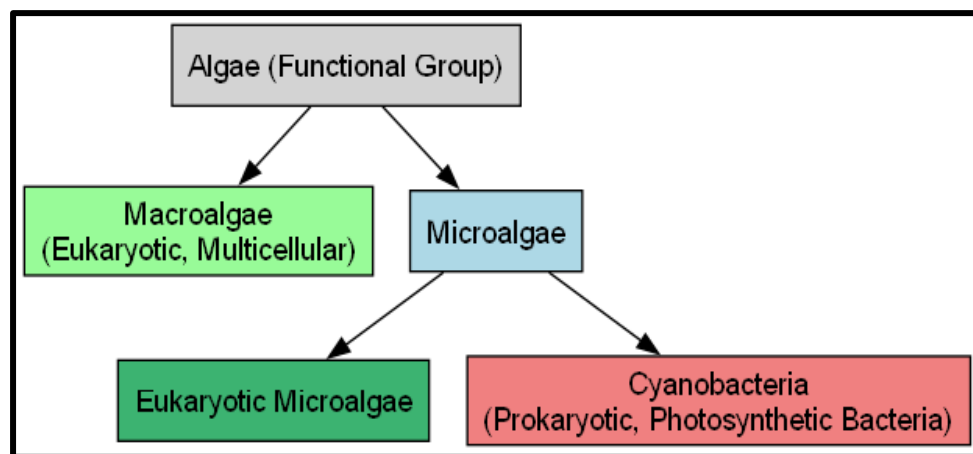


Figure 2. Algae and its major types (Thoré et al., 2023)

Microalgae are incredibly diverse organisms found in many environments, including oceans, freshwater, and moist land areas. As shown in **Figure 2**, they are categorized into categories such as green algae (Chlorophyta), red algae (Rhodophyta), brown algae (Phaeophyta), cyanobacteria, and diatoms. These can be further divided into microalgae (small-sized algae) and macroalgae (large-sized algae). Microalgae itself includes eukaryotic microalgae and prokaryotic microalgae like cyanobacteria (Thoré et al., 2023). The variety among algae species comes from their ability to adapt to different conditions. For example, green algae,

commonly found in freshwater, are closely related to land plants and play an important role in recycling nutrients. Red algae are usually found in deeper ocean waters, where their pigments help them absorb blue light. Brown algae, such as kelp, create underwater forests that serve as habitats for many marine species. These differences in color, shape, and environmental preferences highlight how algae have evolved to thrive in diverse ecosystems (Bouyahya et al., 2024).

1.3. Organization of the thesis

This thesis is structured to address the increasing demand for sustainable antioxidants by investigating indigenous microalga for tocopherol accumulation. Traditionally, antioxidants such as tocopherol have been either chemically synthesized or extracted from plants. However, they have certain limitations, such as the requirement of complex extraction methods and low tocopherol yield. In order to address this problem, the present research explores the potential of 6 indigenous microalgal species to accumulate tocopherol at different phases of growth as well as environmental conditions. Subsequent to primary microalgal screening for the highest tocopherol yield as well as growth, 2 species with contrasting features, i.e., one with high tocopherol yield and another with high growth rate, were chosen for optimization study comprising stress-induced tocopherol production. The current study combines physiological evaluation along with tocopherol estimation to understand the effect of different abiotic factors on tocopherol enhancement. The significance of the present study lies in unraveling the capability of microalgae to act as a scalable and feasible resource of natural antioxidants, thus reflecting the advancement of algal biotechnology for industrial and health applications.

Chapter 2

Literature review

2.1. Antioxidants

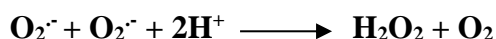
Oxidative stress induces diseases through a complex mechanism involving enhanced production of ROS that flood the body's antioxidant defenses, leading to cellular and molecular damage. The processes through which ROS/RNS induce or regulate apoptosis generally involve receptor activation, caspase activation, Bcl-2 family proteins, and mitochondrial dysfunction (Ryter et al., 2007).

Free radicals are unstable molecules, often described as electron deficient. They require additional electrons to become stable or complete. To achieve this stability, free radicals seek electrons from other molecules in the cell, which in turn makes those molecules unstable (Jamdade & Bodare, 2023). Antioxidants are like superheroes in the movie; they don't capture electrons from healthy cells in our bodies. They provide electrons and become unstable by donating electrons to free radicals or ROS and preventing cell and biomolecule oxidation. Antioxidants balance the production and destruction of free radicals and ROS molecules in the cells. When cells lack sufficient antioxidants to neutralize free radicals, these radicals target other vital molecules, leading to oxidative stress in the body (Pham-Huy et al., 2008).

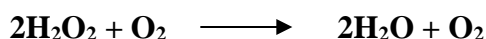
ROS overproduction leads to lipid peroxidation, protein oxidation, and DNA damage. Lipids are essential for cell membrane integrity and functional stability. ROS oxidize polyunsaturated fatty acids in cell membranes, disrupting membrane integrity and generating toxic malondialdehyde (MDA) and hydroxynonenal (4-HNE), further propagating and altering cell signaling. ROS causes carbonylation, nitration, and cross-linking of proteins, leading to loss of function, enzyme inactivation, and aggregation, resulting in disease progression. OS induces

DNA strand break, base modifications, which disrupt gene expression, stimulate apoptosis, and contribute to carcinogenesis and degenerative disease (Ayala et al., 2014).

Currently, many antioxidants and ROS scavenging agents have been explored for their valuable & favorable effects against oxidative stress, such as carotenoids, vitamin E (Tocopherols), flavonoids, etc. (Pizzino et al., 2017). The body uses a complex system of antioxidants to keep a balanced redox state. This includes enzymatic antioxidants such as catalase (CAT), superoxide dismutase (SOD), and glutathione peroxidase (GPx), which actively neutralize ROS molecules. SOD, for instance, transforms superoxide radicals into oxygen and hydrogen peroxide.



CAT breakdowns hydrogen peroxide into H₂O and O₂,



And GPx uses glutathione to reduce peroxide (Bewick et al., 1987). Non-enzymatic antioxidants such as β-carotene, glutathione, vitamins C and E, and minerals function additionally to scavenge free radicals and support enzymatic activities (Irato & Santovito, 2021).

2.2. Algal metabolites as antioxidants

Algae can grow in various water types, including seawater, brackish water, and wastewater. This adaptability, combined with their ability to photosynthesize more efficiently than land plants and their quick growth cycle, makes microalgae a valuable resource for producing important biochemicals. Their growth and composition can be adjusted by modifying the nutrients in their environment or changing physical factors like pH, temperature, light intensity, day-night cycles (Pancha et al., 2014). Specific techniques are used to increase the synthesis of important compounds such as lipids, proteins, carbohydrates, vitamins, and various secondary

metabolites. For instance, reducing nitrogen in their environment effectively boosts these components (Ördög et al., 2012). Interestingly, moderate levels can sometimes lead to better growth and productivity instead of completely removing nitrogen. Other stress factors, like phosphate limitation, salinity, photoperiod, or temperature changes, can also enhance their biochemical properties. Additionally, altering nutrient levels or pH can even change the shape and structure of microalgae (Pancha et al., 2014). This flexibility and productivity make microalgae an exciting option for various applications, including biofuels and healthcare products.

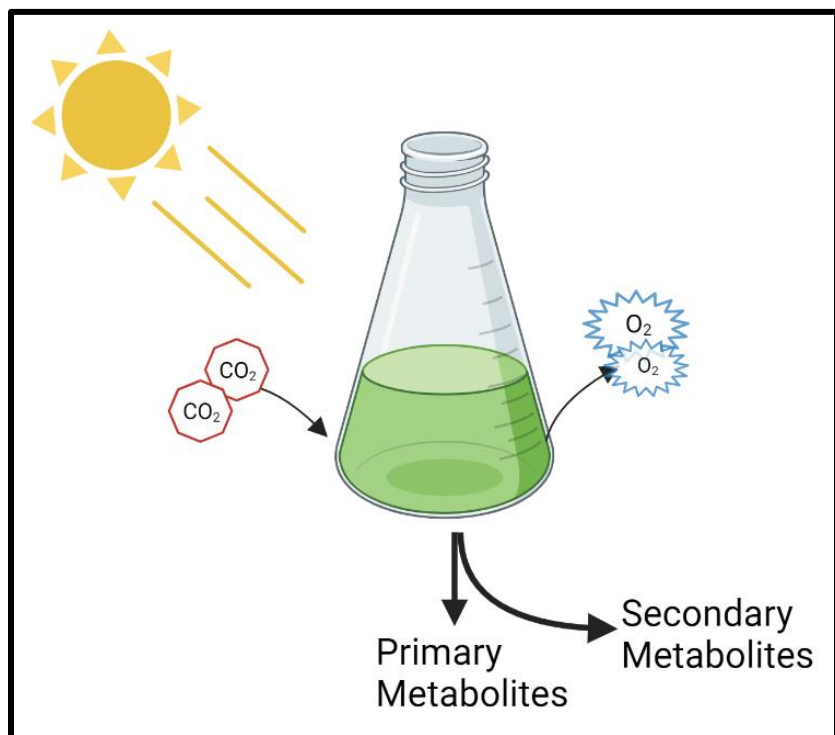


Figure 3. Mechanism of secondary metabolites production

Algae produce various primary and secondary metabolites as shown in **Figure 3**, like isoprenoids, sterols, polyphenols, alkaloids, carotenoids, flavonoids, phycobiliproteins, polyunsaturated fatty acids (PUFA), astaxanthin, docosahexaenoic acid (DHA) and eicosapentaenoic acid (EPA) exhibiting promising biological and nutraceutical activities including

anticancer, antioxidant, antimicrobial, antiviral, anti-allergy, immunomodulatory and anti-inflammatory properties (David et al., 2015; Martins et al., 2014). Some of them are only synthesized and found in plants and algae. Agar from *Gracilaria gigas*, alginate extracted from *Sargassum hystrix*, and sulfated galactofucan from *Padina tetrastrum* show good α -glucosidase inhibitory activity and α -Amylase inhibition activity (Hardoko et al., 2015; Zhan et al., 2022).

Fucoxanthin protects the retina by activating catalase and by reducing oxidative stress induced by high blood glucose levels; it also shows an antidiabetic effect by facilitating GLUT4 transporter expression and translocation in muscles (Martins et al., 2014). Some studies show that the anti-inflammatory role of fucoxanthin is that it decreases inflammatory cytokines associated with insulin resistance (IR). It stimulates and activates the Sirt/ Nrf2 signaling and Akt/Sirt1/FoxO3 α pathway to alleviate oxidative stress in diabetic nephropathy and improve kidney functioning. Fucoxanthin also shows inhibitory activity against α - glucosidase and α -amylase, enzymes involved in carbohydrate digestion. It supports insulin sensitization and combats lipid accumulation in liver cells via Sirt1/AMPK signaling (Bhatti et al., 2022).

2.3. Biochemical classification of algal isoprenoid lipids with emphasis on tocopherols

Terpenoids, also known as prenol lipids or isoprenoids, showcase one of the major significant classes of naturally occurring metabolites in eukaryotes and prokaryotes. On the basis of structure, isoprenoids are basically made up of 5-carbon isoprenes (C₅H₈) unit and are distinguished based on their arrangement and quantity (Gershenzon & Dudareva, 2007). Different types of isoprenoids as shown in **Figure 4**, are known to perform a wide variety of important functions, such as protection from oxidative

stress (tocols), photosynthesis (carotene), electron transport (quinones), and role in membrane structure (polyprenols, etc.) (Vranová et al., 2013).

Tocols, specifically the vitamin E family, are a crucial class of isoprenoids. Tocols are primarily produced in photosynthetic organisms like algae, a few cyanobacteria and plants. Tocols play a critical role in antioxidant defense mechanisms in these organisms, specifically within chloroplasts. Tocopherol refers to a class of eight fat-soluble compounds, consisting of four tocopherols (α , β , γ , δ) and four tocotrienols (α , β , γ , δ). Among them, α -tocopherol is recognized as the most biologically active form, noted for its strong antioxidant and anti-inflammatory effects. It has the potential to prevent chronic diseases. The antioxidant capacity of tocopherols is in the following order: $\alpha > \beta > \gamma > \delta$ (Udaypal et al., 2024).

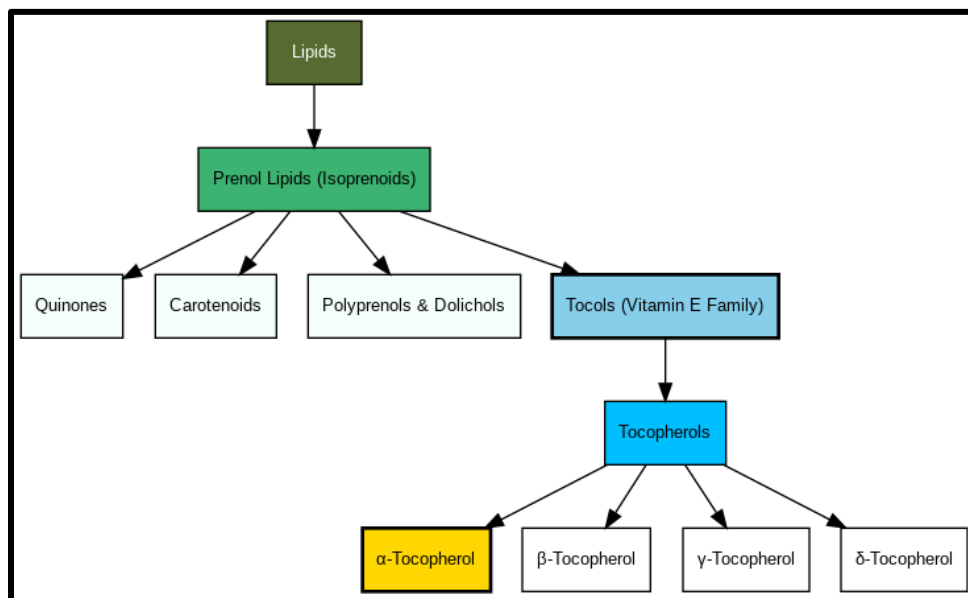


Figure 4. Isoprenoids classification

Tocopherols are a group of organic compounds acting as vitamin E. This name, derived from Greek, reflects its role in reproduction: *tókos* (birth) and *phérein* (to carry), combined with the suffix "-ol," indicating that it is a type of alcohol. These fat-soluble compounds are part of a larger

group called tocopherols, which include tocopherols and tocotrienols. Both categories have four forms: α , β , γ , and δ , all made mainly by plants and algae. Tocopherol biosynthesis involves the integration of precursors from two different metabolic pathways. The chromanol ring of tocopherol is initially formed from homogentisic acid (HGA), which is produced through the shikimate pathway in the cytosol. In contrast, its hydrophobic side chain comes from phytyl diphosphate (PDP), which is generated via the methylerythritol phosphate (MEP) pathway inside the plastids. The enzymatic condensation of HGA and PDP initiates the formation of tocopherol (Lushchak & Semchuk, 2012). Both the SA and MEP pathways serve as upstream contributors to tocopherol production, providing metabolic flux and showing interconnection with the other essential processes such as pigments synthesis and phytohormone's synthesis (T et al., 2017).

Tocopherols and tocotrienols are well-known for their health benefits (Kamal-Eldin & Appelqvist, 1996). They protect against conditions like obesity, heart disease, cancer, neurological disorders like Parkinson's and Alzheimer's, and diabetes. These benefits come from their anti-inflammatory and antioxidant properties. They are also essential in regulating gene expression, supporting the immune system, and facilitating DNA repair processes. While offering even greater therapeutic potential, Tocotrienols are less accessible and more expensive than tocopherols, making tocopherols the more practical choice (Aksoz et al., 2020).

There's increasing demand for natural tocopherols, especially in cosmetics and personal care, because they are more biologically active and have fewer side effects compared to synthetic versions. However, most available tocopherols are synthetic, with only about half the biological activity of natural ones. Natural sources like soybeans, sunflower seeds, tomatoes, and olive oil produce tocopherols, but their yields are low and highly affected by environmental conditions, limiting their large-scale use

(Aksoz et al., 2020). Microalgae offer a sustainable alternative for tocopherol production. They can grow year-round, adapt to various conditions, and don't require farmland. Microalgae yield more tocopherols and provide valuable by-products like carbohydrates, protein, and vitamins, making them economically viable. Current research focuses on improving tocopherol biosynthesis in microalgae, refining extraction methods, and addressing challenges in large-scale production, which could transform the natural tocopherol market. Various studies have reported that microalgae *Tetraselmis* sp. (1981 ± 2.60 mg/100g DW) and *Chaetoceros* sp. (1222 ± 120 mg/100g DW) are major producers of tocopherol among all algal and food sources (Singh et al., 2020; Udaypal et al., 2024).

From a biological perspective, tocopherols work by neutralizing harmful free radicals. Their unique structure allows them to donate a hydrogen atom to reduce free radicals, protecting cells from damage as illustrated in **Figure 5**. Their fat-soluble nature enables them to integrate into cell membranes, shielding them from oxidative stress. Different from tocopherols, tocotrienols exhibit even stronger antioxidant effects by having three double bonds in their structure. However, excessive consumption of tocopherols can be harmful. The recommended daily allowance (RDA) for adults is 15 mg, with an upper safe limit set at 1,000 mg per day (Udaypal et al., 2024). Tocopherols are being explored for their potential in treating various diseases, such as cancer, diabetes, Alzheimer's, and cardiovascular conditions, as well as addressing issues like obesity and skin aging. Tocopherols, especially α -tocopherol, are efficient lipid-soluble antioxidants that protect cell membranes and lipoproteins from oxidative damage by scavenging lipid peroxy radicals by breaking lipid peroxidation chains (Kamal-Eldin & Appelqvist, 1996; Yoshida et al., 2003). This antioxidant property secures cellular integrity and prevents oxidative damage from occurring in various diseases (Jiang, 2014).

Current studies show that tocopherol homologous (α , β , γ , and δ) show differences in their antioxidant capacity and bioavailability. While α -tocopherol is classically considered the most potent and abundant in human tissues, γ and δ - tocopherols exhibit more powerful antioxidants and anti-inflammatory effects in certain model organisms; potentially, it may be due to better scavenging of RNS and modulating cell signaling (Engin, 2009; Saldeen & Saldeen, 2005). Emerging research states the role of tocopherols in gene regulation and cellular signaling. Tocopherols influence the activity of genes related to inflammation, cell division, and programmed cell death, apart from their role as antioxidants. In emerging research, these non-antioxidant effects and roles are gaining focus as crucial mechanisms underlying tocopherol's health benefits (Engin, 2009; Meulmeester et al., 2022).

Clinical studies of α -tocopherol supplementation highlight its therapeutic potential in oxidative-related diseases, yet results are insignificant. While tocopherol reduces lipid peroxidation and improves antioxidant levels in diseases like CVD, diabetes, and neurodegeneration, some large-scale trials report limited or inconsistent outcomes; now it needs a better understanding of dosage, bioavailability, and tocopherol form (Meulmeester et al., 2022). **Table 1** demonstrates different sources of tocopherols along with their yield. The comparison of different tocopherol sources suggests that further research is needed to explore tocopherol producers in a sustainable and feasible manner.

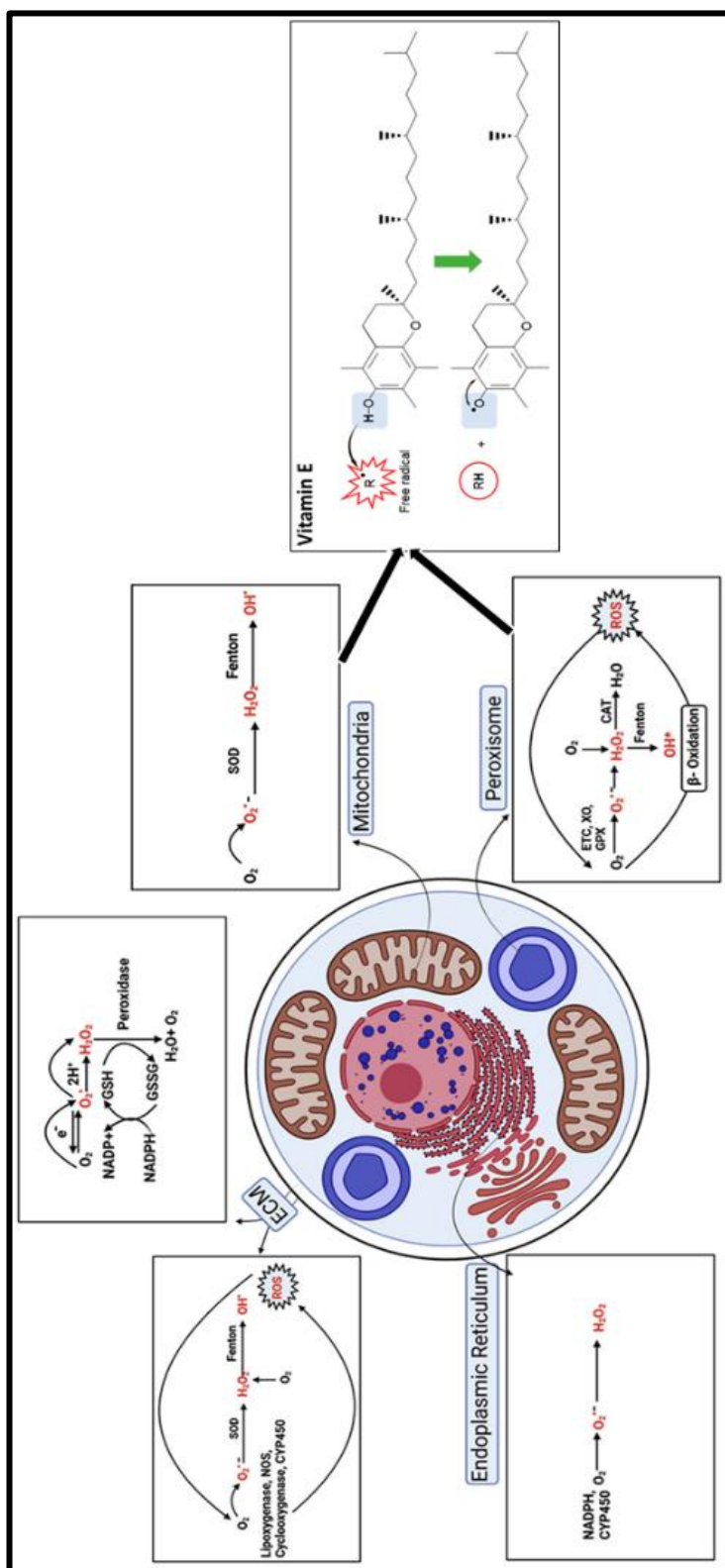


Figure 5. Mechanism of ROS production and destruction (Udaypal et al., 2024)

Table 1. Tocopherol yield of different food groups

Food Group	Description	Average Tocopherol Concentration (mg/100g DW)					References
		α -T	β -T	γ -T	δ -T	Total	
Vegetables	Spinach	1.96 \pm 0.43	ND	0.21 \pm 0.06	ND	2.17 \pm 0.49	(Chun et al., 2006)
	Carrot	0.86 \pm 0.44	0.01 \pm 0.01	ND	ND	0.87 \pm 0.45	
Fruits	Blackberries	1.43 \pm 0.74	0.04 \pm 0.02	1.42 \pm 0.15	0.85 \pm 0.33	3.74 \pm 1.24	(Chun et al., 2006)
	Blueberries	0.58 \pm 0.21	ND	0.38 \pm 0.09	0.02 \pm 0.03	0.98 \pm 0.33	
Nuts	Walnut	1.92 \pm 0.11	ND	36.4 \pm 1.13	35 \pm 0.34	73.32 \pm 1.58	(Melhaoui et al., 2018; Gao et al., 2018)
	Almond	51.7 \pm 0.8	0.29 \pm 0.03	0.9 \pm 0.1	ND	52.89 \pm 0.93	
Dairy	Cheese	50.1	ND	7.1	ND	57.2	(Górnas et al., 2014; Lerch et al., 2015)
	Butter	7.66 \pm 0.15	ND	8.98 \pm 0.21	0.18 \pm 0.02	16.82 \pm 0.38	
Cereals	Rice	1.39 \pm 0.08	0.1	0.36 \pm 0.01	0.017	1.86 \pm 0.09	('Tremmel-Bede et al., 2022);(Nguyen Huynh Phuong et al., 2021)
	Wheat	0.63	0.34	0.018	ND	0.98	
Vegetable oils	Soyabean oil	11.53	ND	67.55	26.16	105.24	(Wu et al., 2020)
	Sunflower oil	71.84	ND	2.15	0.27	74.26	
Microalgae	<i>Tetraselmis</i> sp.	170 \pm 20	111 \pm 40	1700 \pm 200	ND	1981 \pm 260	(Carballo-Cárdenas et al., 2003)
	<i>Chaetoceros</i> sp.	89 \pm 10	83 \pm 10	1050 \pm 100	ND	1222 \pm 120	

2.4. Factors affecting algal tocopherol production

Various factors affect the growth and accumulation of tocopherol in the algae, such as environmental factors like light intensity, photoperiods, temperature, salinity, and genetic and biochemical factors like CO₂ and N₂ that regulate its biosynthesis within algal cells. Light plays an essential role in tocopherol biosynthesis, as tocopherols are located mainly in the membranes of thylakoids and plastids involved in photosynthesis. Higher intensity can increase oxidative stress, promoting algae to enhance tocopherol accumulation for photoprotection and antioxidant defense (Ljubic et al., 2021; Munné-Bosch, 2005). Likewise, temperature can influence tocopherol content by affecting algae's metabolic, enzymatic activities, and oxidative stress levels. High temperature tends to increase oxidative damage, enhancing ROS generation, which can trigger increased tocopherol synthesis to scavenge ROS and protect cellular components, leading to a rise in tocopherol accumulation as a protective mechanism for ROS tolerance. Extreme temperature may impair biosynthesis and metabolic efficiency (Durmaz et al., 2008; Soengas et al., 2018).

Nitrogen limitation is also a well-studied factor that promotes tocopherol accumulation in algae. Under nitrogen starvation, oxidative stress increases due to metabolic imbalance and reduced cellular growth. This stress condition stimulates the biosynthesis of tocopherols and other antioxidants as a defense mechanism. For example, nitrogen limitation in *Scenedesmus* sp. and *Nannochloropsis* sp. significantly enhances α -tocopherol content; it may be at the cost of biomass and growth rates (Durmaz, 2007; Ghosh et al., 2025). Changes in salinity induce osmotic stress and ROS production in algae; as a result, it leads to enhanced tocopherol synthesis as a defense mechanism. Marine algae like *Dunaliella* sp. show marked increases in tocopherol under high salinity. Similarly, pH fluctuations can affect enzymatic activities involved in tocopherol biosynthesis (Carballo-Cárdenas et al., 2003). In a nutshell, abiotic stress

factors have different effects on the accumulation of tocopherol as depicted in **Table 2**.

Tocopherol content does not always remain the same and changes across different growth phases. Typically, tocopherol accumulation peaks during the late exponential or stationary phases, with higher oxidative stress due to nutrient depletion and metabolic shifts. Harvesting in optimal phases maximizes tocopherol yield (Mudimu et al., 2017). Tocopherol biosynthesis capacity significantly varies among algal species based on their genetic diversity and metabolic diversity. Genetic regulation of biosynthesis enzymes and precursor supply directly influences the tocopherol level. *Tetraselmis* sp, *Euglena gracilis*, and *Dunaliella tertiolecta* are well known for relatively high tocopherol content (Mokrosnop et al., 2016).

Table 2. Factors affecting algal tocopherol production

Factor	Effect on Tocopherol Accumulation	References
Light Intensity and Quality	Increased light induces oxidative stress, affect tocopherol production	(Ljubic et al., 2021)
Temperature	Moderate heat enhances tocopherol biosynthesis via ROS	(Soengas et al., 2018)
Nutrient Availability	Nitrogen limitation strongly promotes tocopherol accumulation	(Ghosh et al., 2025)
Salinity and pH	Salt stress and pH variations stimulate antioxidant defense	(Carballo-Cárdenas et al., 2003)
Pollutants and Heavy Metals	Toxic stress raises ROS, triggering tocopherol synthesis	(Ercal et al., 2001)
Growth Phase	Late exponential/stationary phases show higher tocopherol	(Mudimu et al., 2017)
Species and Genetics	Genetic diversity dictates biosynthetic capacity	(Mudimu et al., 2017)
Biosynthetic Enzyme Regulation	Stress signals modulate enzyme activity and tocopherol levels	(Mokrošnop et al., 2016)

Chapter 3

Hypothesis and objectives

3.1. Hypothesis

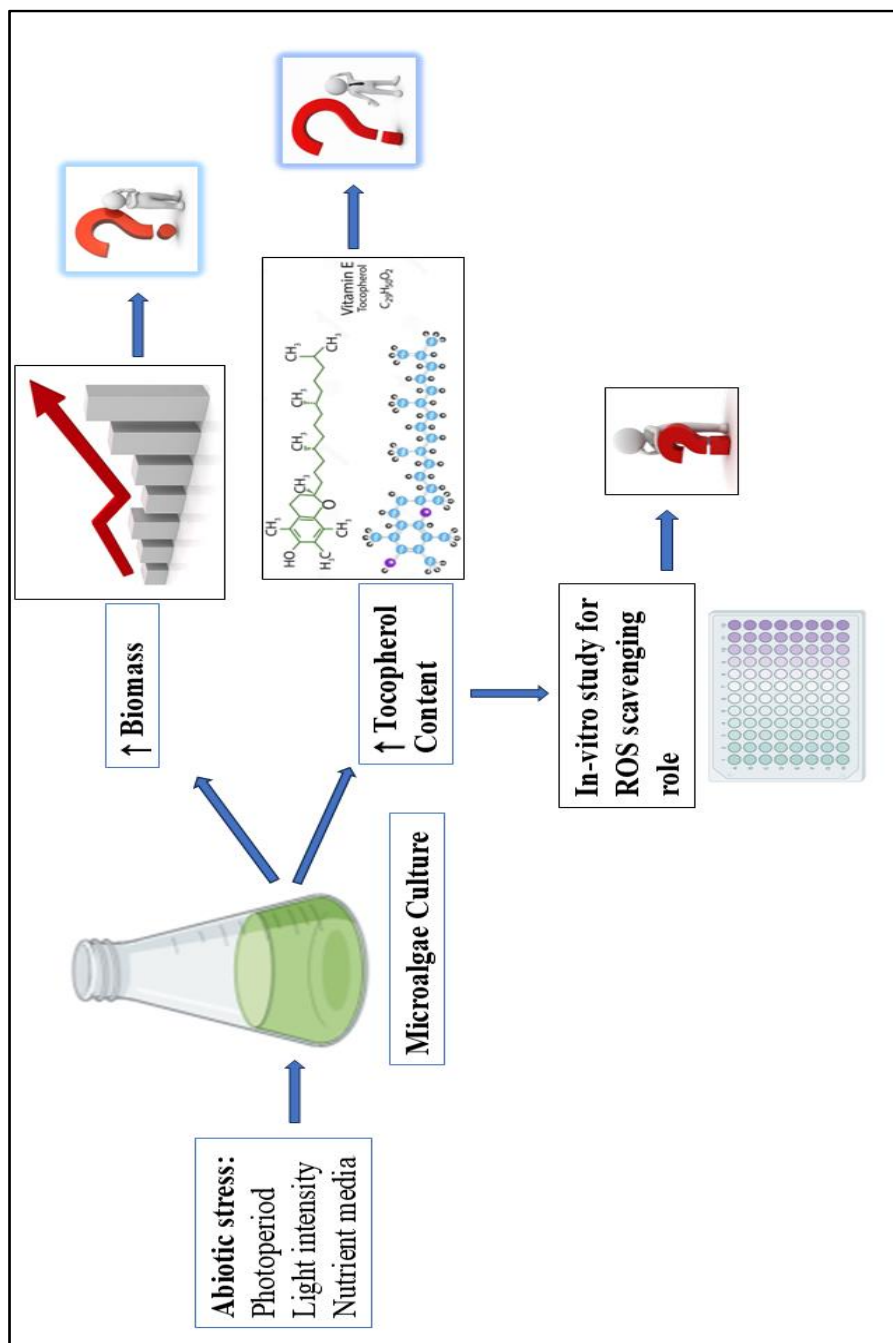


Figure 6. Diagrammatic representation of hypothesis

The increment in the occurrence of oxidative stress-induced disorder highlights the urgent need for efficient and sustainable antioxidant resources. Vitamin E member, tocopherols, have been known to be the most capable natural antioxidant owing to their potential to counteract reactive oxygen species (ROS) and obstruct the peroxidation of lipids. Though terrestrial plants are the traditional source, the tocopherol extraction from these natural sources has limitations in terms of agricultural land, low yield, and seasonal variability, thus preventing the continuous availability of commercial applications. These constrictions necessitate the investigation of scalable and viable substitutes for tocopherols.

Microalgae is a promising and underused source of antioxidant tocopherol biosynthesis. Various factors, such as the ability to adapt to environmental stress, rapid growth rate, and metabolic versatility make them attractive candidates for augmenting the biosynthesis of secondary metabolites like tocopherols under optimized environmental conditions. Initial investigations suggest that the accumulation of tocopherols in microalgae can be regulated significantly by various environmental factors such as salinity, light intensity, photoperiod, nutrient stress, etc. However, comparative investigations are scarce based on the interaction of diverse algal species and stress conditions for tocopherol production.

On the basis of the above-stated problem, the present investigation hypothesizes (**Figure 6**) that certain microalgal species, when exposed to defined abiotic stressful combinations, can augment their tocopherol production. The study focuses on determining the potential of certain species, showcasing the superior tocopherol content along with improved antioxidant potential. The rationale of the research depends on exploiting stress-induced metabolic fingerprints to unravel high tocopherol-yielding and robust algal candidates for the biosynthesis of tocopherol. The research aims to support the advancement of microalgae as a sustainable and feasible

alternative biological source and promote the replacement of agricultural and chemically limited antioxidants in the field of nutraceuticals and health.

3.2 Objectives of the study

To summarize the aforementioned hypothesis and rationale, the following is the major objective of the study:

“Unraveling the tocopherol production potential of microalgae for antioxidant applications.”

To accomplish the major objective, current research has been divided into the following minor objectives:

1. Characterization & Screening of Microalgal Species for High Tocopherol Production.
2. Investigating the Impact of Abiotic Factors on Microalgae for Enhanced Tocopherol Production.
3. Estimating In-vitro Hydrogen Peroxide Scavenging Activity of Tocopherol.

Chapter 4

Materials and methodology

4.1. Materials

4.1.1. Microalgal species

For the experimental study, six native microalgal species were selected. These are IMMA 11, IMMA 12, IMMA 13, IMMA 14, IMMA 15, and IMMA 16. Further based on cell size IMMA 12 and IMMA 15 were categorized as small-sized microalgae, while the remaining species were classified as large-sized microalgae.

4.1.2. Experimental chemicals and solvents

The cultivation of these six microalgal species was carried out using BG-11 nutrient broth (Himedia) and 1.5 % agar powder (Himedia) was used for plating purposes. The composition of BG-11 media is listed in **Table 3**. Various organic solvents were used in the different stages of experiment which include - Methanol (MeOH), Acetonitrile (ACN), Hexane, Acetone, Dichloromethane (DCM) which were supplied by Merck and Ethanol (Labnol).

Table 3. Composition of BG-11 media

S. No.	Components	g/L
1	Sodium nitrate (NaNO_3)	1.5
2	Magnesium sulphate (MgSO_4)	0.036
3	Dipotassium hydrogen phosphate (K_2HPO_4)	0.031
4	Calcium chloride dihydrate ($\text{CaCl}_2 \cdot 2\text{H}_2\text{O}$)	0.036
5	Sodium carbonate (NaCO_3)	0.02
6	Disodium magnesium EDTA	0.001

7	Citric acid	0.006
8	Ferric ammonium citrate	0.006
9	Trace Elements:	
	Boric acid (H_3BO_3)	0.028
	Manganese chloride tetrahydrate ($\text{MnCl}_2 \cdot 4\text{H}_2\text{O}$)	0.018
	Zinc sulphate (ZnSO_4)	0.002
	Sodium molybdate dihydrate ($\text{Na}_2\text{MoO}_4 \cdot 2\text{H}_2\text{O}$)	0.039
	Copper sulphate pentahydrate ($\text{CuSO}_4 \cdot 5\text{H}_2\text{O}$)	0.007
	Cobalt nitrate ($\text{Co}(\text{NO}_3)_2$)	0.004

4.2. Methodology

4.2.1. Media preparation and microalgal culture maintenance

All six microalgal strains used in this study were previously isolated from various locations in Indore and were taxonomically identified by the National Collection of Industrial Microorganisms (NCIM), Pune. The BG-11 nutrient medium was prepared according to standard protocol, with the required quantity, measured using a Shimadzu ATX224R analytical balance. The medium's pH was maintained at 7.2 ± 0.2 by adding either 1 M NaOH or 1 M HCl, depending on the requirement. (Systronics μ pH System 361).

Subsequently, 100 mL of the prepared medium was dispensed into 250 mL Erlenmeyer flasks, were closed with cotton plugs and sterilized in an autoclave at 121 °C and 15 psi for 20 minutes. All supporting labware, including 15 mL and 50 mL centrifuge tubes, measuring cylinders, pipette tips, flasks, and distilled water, were also sterilized to prevent contamination.

Following sterilization, each Erlenmeyer flask containing 100 mL of medium was inoculated with 1 mL of the respective stock microalgal culture. These flasks served as seed cultures and were maintained under control conditions in a culture room, with a 12:12-hour light-dark photoperiod, light intensity of 3000 ± 500 Lux (measured using a Lutron LX-101A Lux meter), and temperature maintained at 27 ± 2 °C.

Microalgal cultures in their logarithmic growth phase were sub-cultured into fresh medium, standardized until an optical density of 0.2 was achieved at 680 nm ($OD_{680 \text{ nm}}$). All culture handling and transfers were carried out under a laminar airflow cabinet (Microfilt Technologies LLP) to maintain aseptic conditions throughout the process.

4.2.2. Morphological characterization

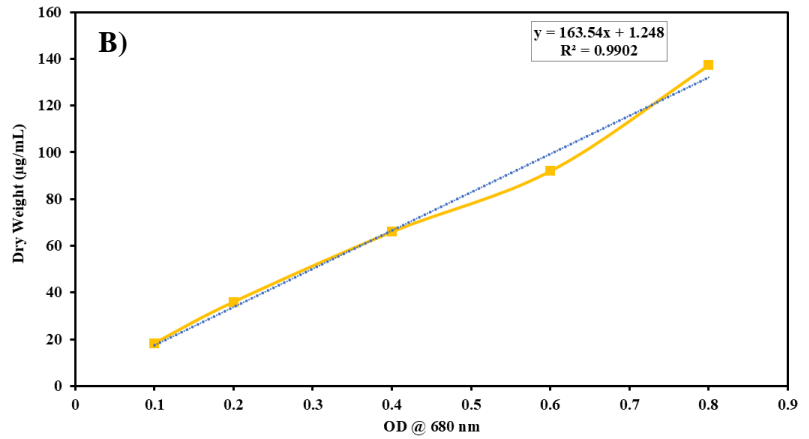
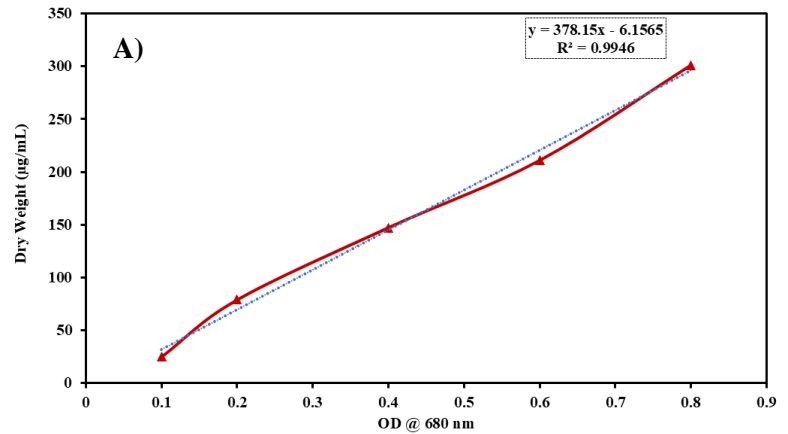
Morphological characterization of the microalgal strains was carried out using a light microscope (Olympus CKS53). A single drop of each culture was placed on a clean glass slide and examined under 40x magnification to assess cell size and confirm culture purity. This step ensured that the microalgal samples were free from cross-contamination prior to their use in subsequent growth and biochemical analyses.

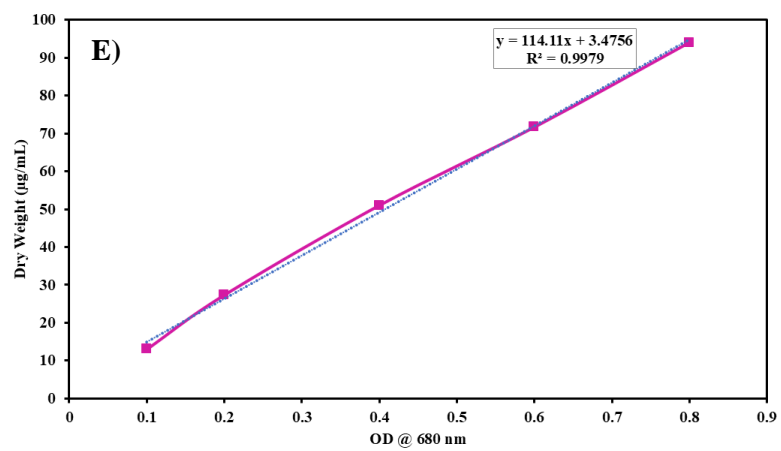
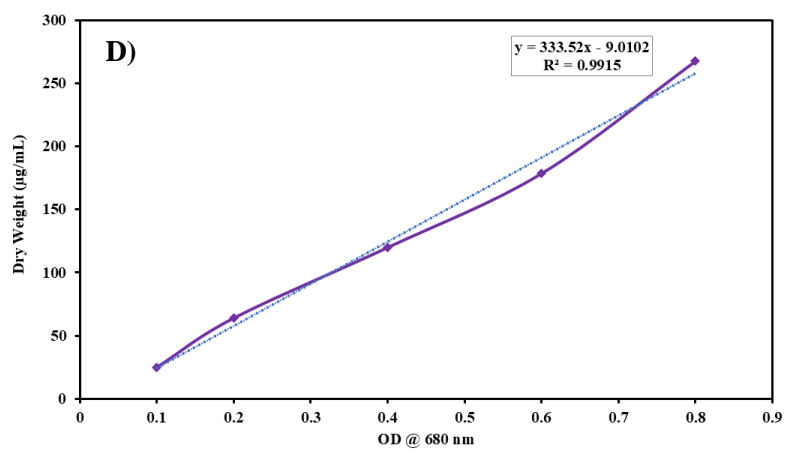
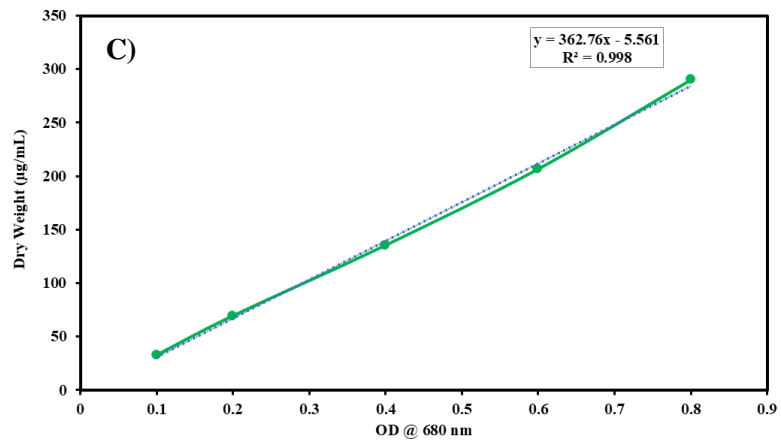
4.2.3. Evaluating algal biomass concentration

The experiment was set up in triplicate of all six species with 0.2 OD (Optical Density), and OD was taken at 680 nm ($OD_{680 \text{ nm}}$) for growth estimation (PerkinElmer Lambda 365). Optical density of cell was measured at every 48 hours and growth curve plotted based on OD of microalgae.

Microalgal growth was monitored at regular intervals, and biomass was harvested by centrifugation at 7500 RPM for 5 minutes (Eppendorf 5430 R centrifuge). The collected biomass was then freeze-dried through lyophilization to obtain the dry weight. To determine the biomass,

corresponding to specific optical densities (OD), known volumes of culture—calculated based on the quantity needed to inoculate 100 mL of medium were taken from the stock cultures. These samples, corresponding to OD values of 0.1, 0.2, 0.4, 0.6, and 0.8, were lyophilized (Alpha 1-2 LD Plus, lyophilizer), and the resulting dry weights were recorded.





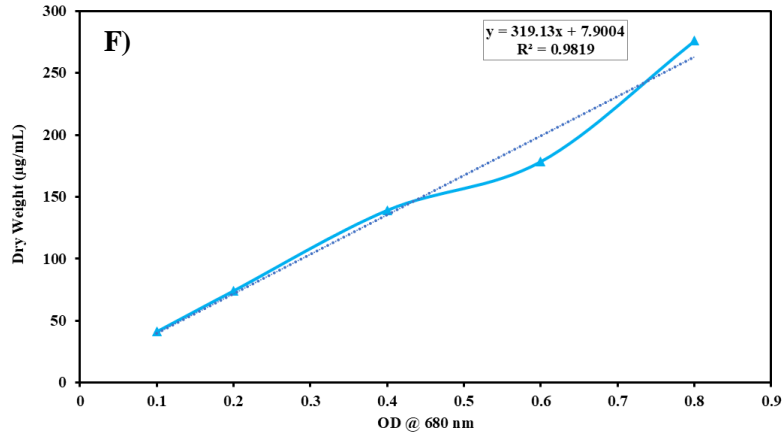


Figure 7 A, B, C, D, E, F shows the relation between OD and dry weight of the six microalgal species under study

4.2.4. Cell kinetics

Biomass production, expressed in micrograms per milliliter (µg/mL) and denoted as DW (Dry Weight) in **Figure 7 A, B, C, D, E, F**, six microalgal species IMMA11, 12,13,14,15,16 respectively, was determined using a calibration curve generated from the linear relationship between absorbance (OD_{680 nm}) and corresponding dry biomass measurements. Since cell growth is closely related to biomass accumulation, this approach provided a reliable basis for the observation of microalgal growth.

To further understand growth dynamics, three key parameters, i.e., biomass productivity, specific growth rate and the cell division time were calculated by using the equations i, ii, and iii, as follows. These parameters were derived using standard models described by (Guillard et al., 1973).

Biomass productivity (P) indicates the rate at which biomass accumulates over time and was calculated using the formula:

$$P = (X_2 - X_1) / (T_2 - T_1) \quad \text{----- (i)}$$

Where:

P = biomass productivity ($\mu\text{g/mL/day}$)

X_1 and X_2 = biomass levels measured at time intervals T_1 and T_2 , respectively.

To quantify how quickly the cells were dividing, the specific growth rate (μ) was determined using the natural log of the ratio between final and initial cell densities:

$$\mu = (\ln (N_t / N_0)) / (T_t - T_0) \quad \text{----- (ii)}$$

Where:

μ = specific growth rate (per day)

N_0 = initial cell concentration

N_t = cell concentration after a defined time period

The average time required for the cell population to double (division time) was calculated using the formula:

$$\text{Division time} = 0.69 / \mu \quad \text{----- (iii)}$$

Where:

0.69 is the natural logarithm of 2

μ = specific growth rate

4.2.5. Pigment estimation

The quantification of chlorophyll a, chlorophyll b, total chlorophyll, and carotenoids was performed using a method adapted from (Lichtenthaler, 1987). To begin with, 1 mL of the microalgal culture was transferred into a microcentrifuge tube (MCT). The sample was subsequently centrifuged at 10,000 RPM for 10 minutes at 10 °C. After

removing the supernatant, the pellet was carefully washed with distilled water and centrifuged again under the same conditions to eliminate any remaining media components. Following the second centrifugation, the supernatant was discarded, and 1 mL of methanol was added to the pellet.

The MCT containing pellet and methanol was wrapped in aluminium foil to protect it from light and subjected to an incubation at 45 °C for 24 hours to ensure thorough extraction of pigments. Following incubation, the sample was vortexed for 1 minute to ensure uniform mixing. It was then centrifuged again at 10,000 rpm for 10 minutes at 10 °C. The clear greenish supernatant, now containing the extracted pigments, was carefully transferred to a fresh MCT. The absorbance of the pigment extract was recorded at four wavelengths: 470 nm, 652 nm, 665 nm, and 750 nm using a spectrophotometer. Readings at 750 nm were used to correct for turbidity, and the absorbance values at the other wavelengths were used to determine the concentrations of chlorophyll a, chlorophyll b, and carotenoids based on the equations outlined by (Lichtenthaler, 1987).

$$\text{Chlorophyll a; Chl a } (\mu\text{g/ml}) = 16.72 * A_{665.2} - 9.16 * A_{652.4}$$

$$\text{Chlorophyll b; Chl b } (\mu\text{g/ml}) = 34.09 * A_{652.4} - 15.28 * A_{665.2}$$

$$\text{Total Chlorophyll (CHL) } (\mu\text{g/ml}) = \text{Chl a} + \text{Chl b}$$

4.2.6. Tocopherol estimation

Tocopherol extraction and quantification were performed following the method outlined by Paliwal and Jutur (2021), with slight modifications. Initially, around 5 mL of algal biomass was disrupted with glass beads (425–600 μm , Sigma Aldrich, USA) in 500 μL of 100% ice-cold ethanol through bead beating. The disruption was carried out intermittently over a total duration of 18 minutes to ensure thorough cell lysis. After centrifugation, 400 μL of the resulting supernatant was collected and mixed with 500 μL of n-hexane and 100 μL of Milli-Q water. This mixture was then vortexed for approximately 4 minutes to promote efficient phase separation. Then, the mixture was centrifuged at 10,000 RPM for 10 minutes at 10 $^{\circ}\text{C}$. The n-hexane layer, containing the tocopherol fraction, was carefully separated and evaporated under a nitrogen gas stream. The dried extract was subsequently reconstructed in 100 μL of a dichloromethane and methanol mixture (2:1, v/v). For analysis, the samples were transferred into GC vials and subjected to HPLC using a Prominence-I LC-2030C 3D PLUS system (Shimadzu, Japan) shown in **Figure 8** fitted with C18 column (15 cm \times 4.6 mm, 5 μm ; Supelco Analytical, USA), The temperature was maintained at 30 $^{\circ}\text{C}$ during the process. Chromatographic separation was performed under isocratic conditions using a binary mobile phase of acetonitrile and methanol in a 60:40 (v/v) ratio, with a flow rate of 0.6 mL/min. Tocopherol was detected using fluorescence detector, with excitation and emission wavelengths set at 297 nm and 330 nm, respectively. Quantification was done by comparing the retention times and peak areas of the samples to those of a standard tocopherol (Sigma-Aldrich, USA) and the tocopherol rich microalgal extract shown in **Figure 9**, based on previously prepared calibration curve.



Figure 8. Prominence-i, LC-2030C 3D PLUS HPLC equipped with a fluorescence detector (RF-20A) CIF, BSBE, IIT Indore)

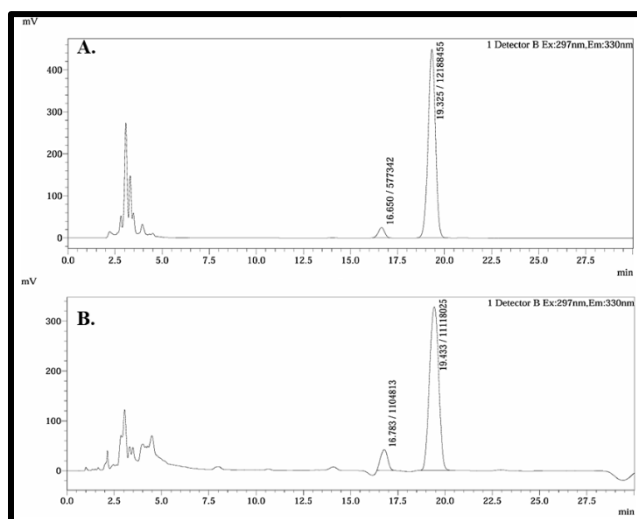


Figure 9. Chromatogram A) α -tocopherol standard peak (10 ppm);
B) Microalgal α -tocopherol rich extract peak

4.2.7. Hydrogen peroxide scavenging activity

The hydrogen peroxide scavenging ability of the extracts was evaluated based on the method defined by (Nabavi et al., 2009) with minor modifications. A crude extract of IMMA14 sp. (400 ng/mL), containing about 25.69 $\mu\text{g/mL}$ of tocopherol and dissolved in DMSO, was mixed with

60 μL of 4.8 mM hydrogen peroxide. The mixture was left to incubate at room temperature for 10 minutes in the dark, after which the absorbance was recorded at 230 nm using a UV-Visible spectrophotometer. Thiamine, a recognized antioxidant, was used as a positive control at the same concentration (400 ng/mL), and its absorbance at 230 nm was recorded under the same experimental conditions. The percentage of hydrogen peroxide scavenged by the extract was calculated and compared with the activity observed in the positive control. The hydrogen peroxide scavenging percentage was calculated using the formula:

$$\% \text{ Scavenged } [\text{H}_2\text{O}_2] = [(A_0 - A_1)/A_0] \times 100,$$

Where, A_0 represents the absorbance of the control (hydrogen peroxide without sample), and A_1 is the absorbance with the extract or standard compound.

4.2.8. Imaging by field emission scanning electron microscopy (FE-SEM)

About 10 μL of the samples were taken onto diamond-cut glass slides and allowed to air-dried overnight. After drying the slides were mounted on stubs by using conductive carbon tape. The mounted samples were then placed in a vacuum chamber and sputter coating of gold was applied to improve the surface conductivity. with a thin layer of gold to enhance the surface conductivity. The stubs were then loaded inside the vacuum chamber of the microscope (FE-SEM Supra 55, Carl Zeiss) and micrographs were captured at a magnification range of 1 K to 5 K.

4.3. Workplan

Based on morphological characteristics, visual observations, and growth parameters, two microalgal species—IMMA 12 and IMMA 14 — were selected for further investigation into their responses to various abiotic stress conditions. Species IMMA 12 demonstrated the highest growth rate, and exhibited a relatively smaller cell size, whereas species IMMA 14 showed the highest tocopherol production among all the strains analyzed. The workflow is further explained in **Figure 10**.

4.3.1. Experimental setup and workplan for understanding the effect of abiotic factor combination on IMMA 12:

To investigate the effects of abiotic factors, three abiotic factors were tested: light intensity (3,000, 9,000, and 15,000 Lux), photoperiod (12:12, 16:8, and 24:0 hours light: dark), and salinity using NaCl (50 mM, 150 mM, and 250 mM). All 27 resulting treatment combinations were set up in triplicate to ensure biological reproducibility, bringing the total number of experimental flasks to 81. In addition, three control flasks were maintained, each inoculated with a 14-day-old mother culture in its logarithmic growth phase. **Figure 11** depicts the IMMA 12 experimental flasks in the culture room.

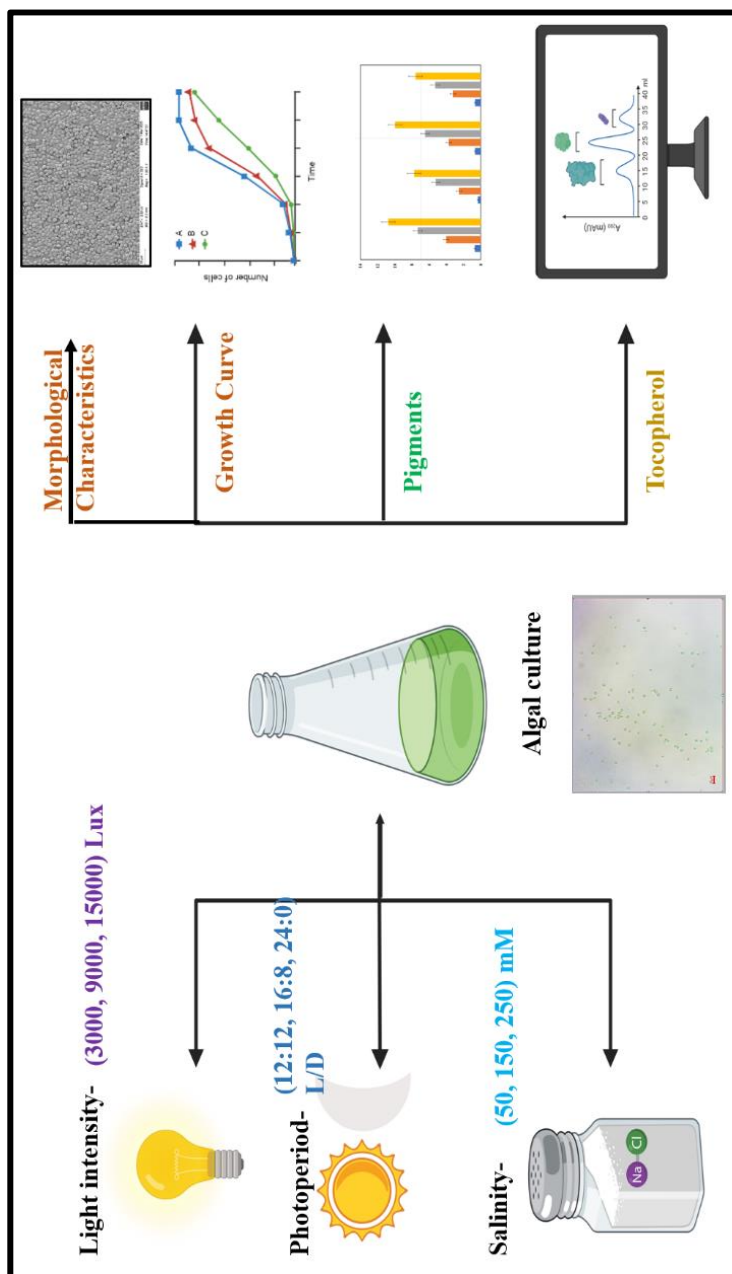


Figure 10. Experimental work plan with algal species for morphological, growth and biochemical characterization



Figure 11. Experimental flasks of microalgae, IMMA 12 under abiotic factor conditions in the BG 11 media

Initial OD readings were recorded on day zero to validate inoculum consistency and to serve as a baseline for growth comparisons. A detailed schematic of the experimental layout is provided in **Figure 12**. Given that growth kinetics indicated a significantly higher growth rate in species IMMA 12, samples were taken from this strain on the 14th and 21st days. Samples were also withdrawn for pigment and tocopherol analysis.

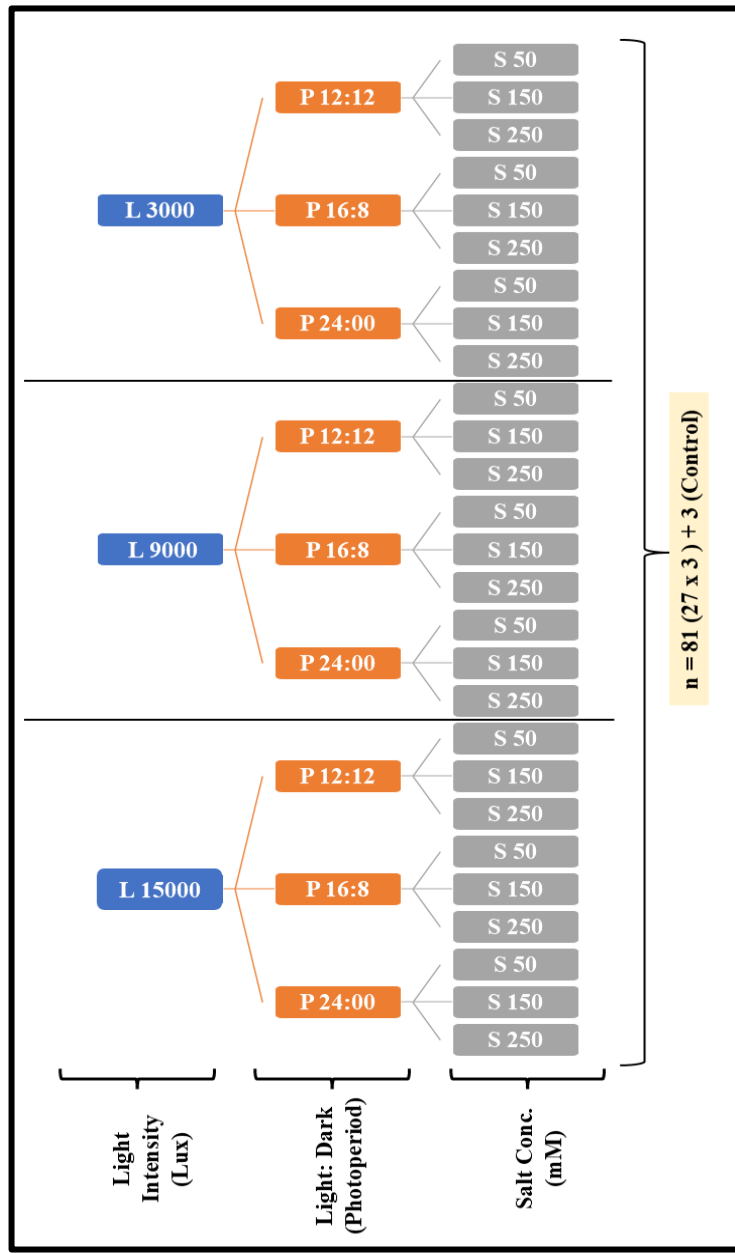


Figure 12. Diagrammatic representation of combination of abiotic factors in experimental flasks of IMMA 12

4.3.2. Experimental setup and workplan for understanding the effect of abiotic factors combination on IMMA 14:

A similar experimental setup was employed for the IMMA 14 strain using the same three abiotic factors—light intensity (3,000, 9,000, and 15,000 Lux), photoperiod durations (12:12, 16:8, and 24:0 hours light:

dark), and salinity adjusted with NaCl (50 mM and 150 mM) represented in **Figure 13**. This resulted in a total of 18 treatment combinations.

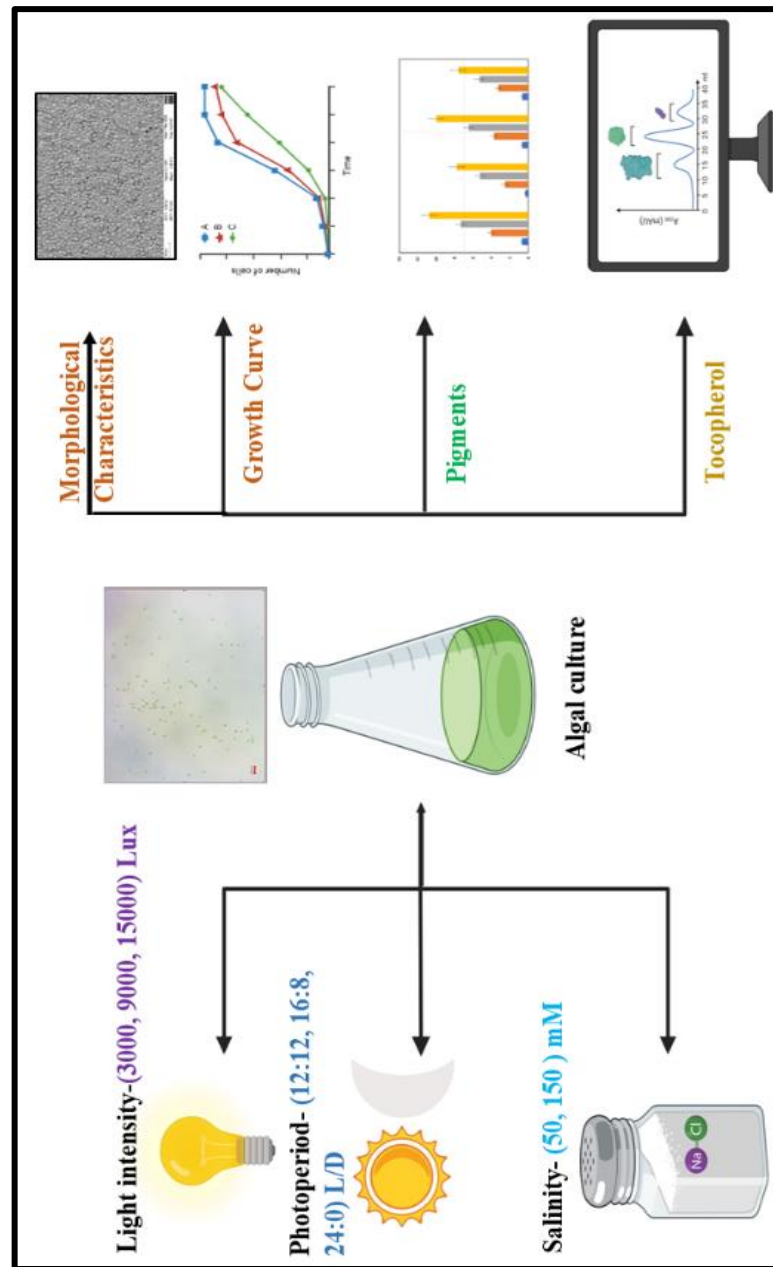


Figure 13. Experimental work plan with algal species for morphological, growth and biochemical characterization

Each treatment was carried out in triplicate to ensure biological consistency, amounting to 54 experimental flasks. Additionally, three

control flasks were maintained, bringing the total number of cultures to 57. A detailed schematic of experimental design is shown in **Figure 14**. Considering the larger cell size and early stationary phase of IMMA 14 and its notable capacity for tocopherol production, culture samples were collected on the 7th and 14th days for pigments and tocopherol analysis.

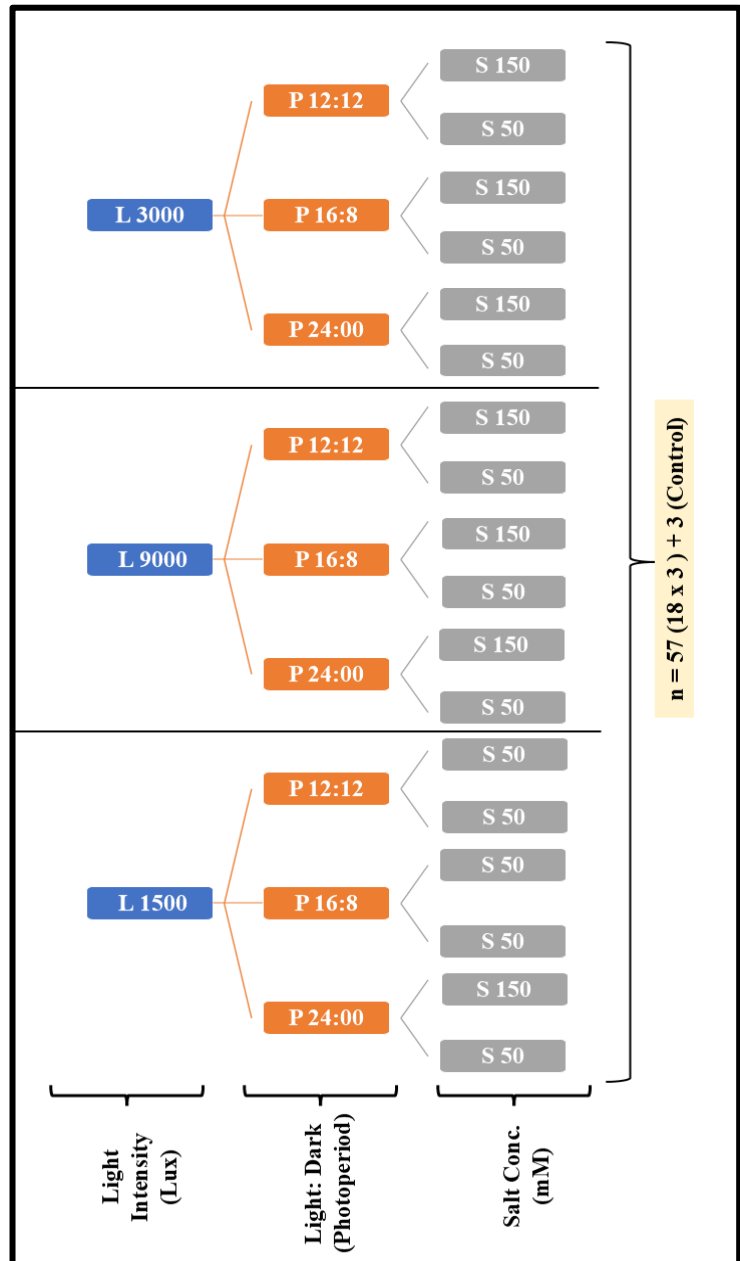


Figure 14. Diagrammatic representation of combination of abiotic factors in experimental flaks of IMMA 14

Chapter 5

Results and discussion

5.1 Characterisation of native microalgal species

5.1.1 Morphological characterisation of native microalgal species

The Morphological characterization of all six species revealed that they are single celled, photosynthetic, green algae member of Chlorophyceae class of Chlorophyta division. They show distinct morphological features, containing pyrenoids & fat bodies (**Figure 15**). Notable, the size of cells in the species IMMA 12 ranges from (1.4 - 1.8 μm), and IMMA 15 ranges from (1.8 - 2.2 μm) which are relatively smaller in comparison to the other four species, IMMA 11 (~6-10 μm), IMMA 13 (~8-10 μm), IMMA 14 (~8-10 μm), and IMMA 16 (~6-8 μm) (**Figure 15**).

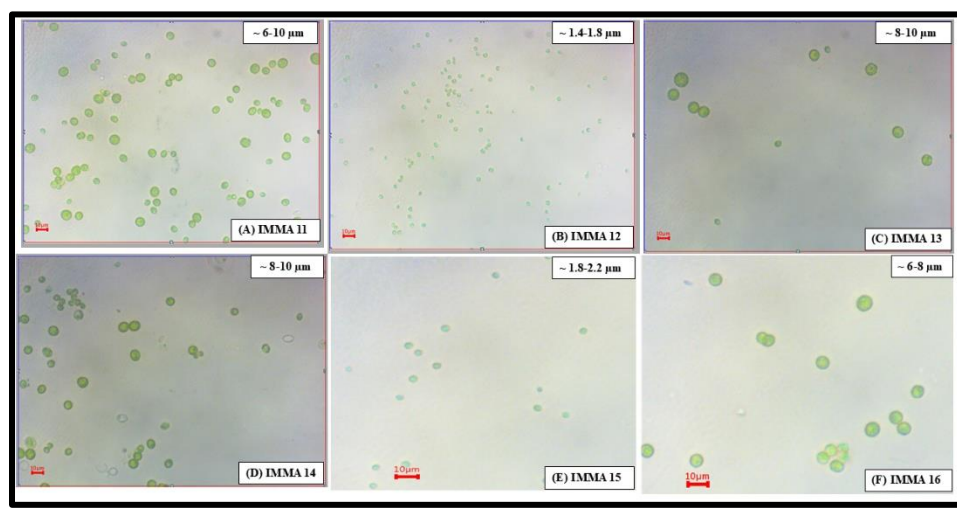


Figure 15. Depicting the different morphology shape and size of native microalgal species (A) IMMA 11, (B) IMMA 12, (C) IMMA 13, (D) IMMA 14, (E) IMMA 15, (F) IMMA 16

5.1.2 Growth characterization of microalgal species

The growth characterization of six species was performed using spectrophotometric data of the biological replicates, in growth curve it can

be clearly seen that the lag, log and stationary phase. In lag phase cell try to adopt in new environment, hence divide slowly, In log phase cells multiply rapidly hence grow exponentially, due to depletion of nutrient in media growth rate slow down. In **Figure 16** IMMA 12 exhibited the highest growth rate as indicated by OD₆₈₀ measurements (yellow line). Following it, IMMA 15 (pink line), IMMA 11 (red line), IMMA 16 (blue line), IMMA 13 (green line), and IMMA 14 (purple line) shows the lowest growth rate.

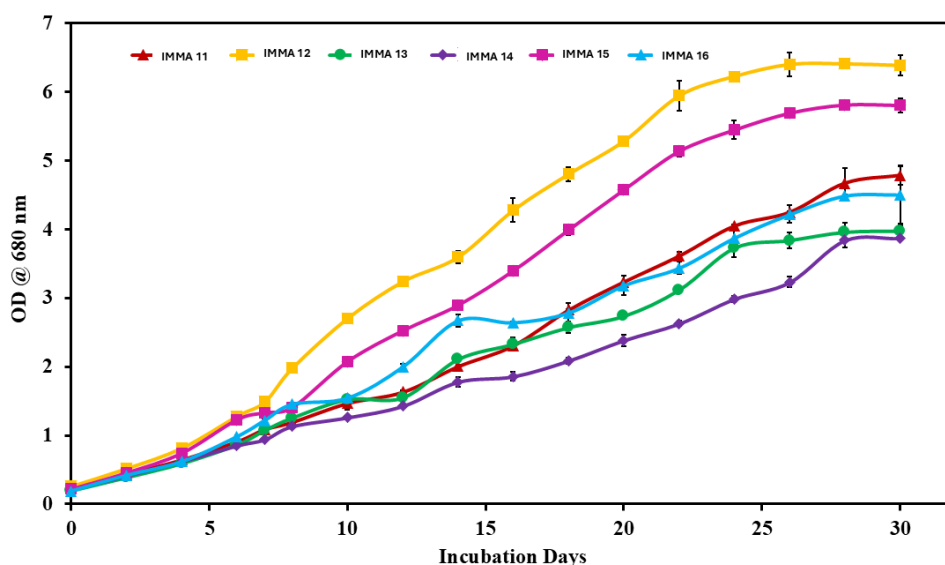


Figure 16. The growth curve depicting the growth characteristic of 6 native microalgal species

5.1.3 Biomass accumulation in microalgal species

Biomass increases consistently over time for all species. Maximum biomass is generally reached at 28 days for each species. In **Figure 17** IMMA 11 shows the highest biomass production at 28 days (1760 ± 80 $\mu\text{g/mL}$), making it the most productive species. IMMA 13 and IMMA 16 also show high biomass at 28 days (1430 ± 49 $\mu\text{g/mL}$), and (1440 ± 6.4 $\mu\text{g/mL}$) respectively indicating strong growth potential. IMMA 15 has the lowest biomass yield throughout the time points, reaching below ($1440 \pm$

6.4 $\mu\text{g/mL}$) at day 28. From day 21 to 28 biomass continues to increase, but the rate of accumulation is low, is suggesting the nearing stationary phase.

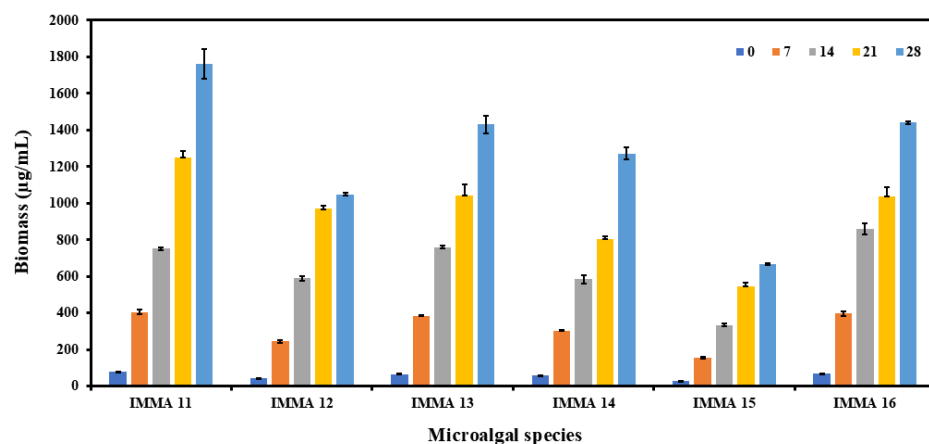


Figure 17. The graph depicts the biomass accumulation of the 6 different native microalgal species at 5 different time point

5.1.4 Cell kinetics of microalgal species

Table 4. Microalgal growth kinetics at log phase

	IMMA 11	IMMA 12	IMMA 13	IMMA 14	IMMA15	IMMA 16
Specific growth rate (μ) (Day)	0.16	0.21	0.17	0.15	0.20	0.19
Division time (day)	4.42	3.32	4.09	4.54	3.35	3.68

The **Table 4** presents the specific growth rate and division time of six native microalgal species (IMMA 11 to IMMA 16) during the logarithmic (log) growth phase. Over time, the specific growth rate tends to decline, reflecting a gradual slowdown in cell proliferation as the culture ages. IMMA 12 exhibited the highest specific growth rate among the isolates on

day 14 ($\mu = 0.21/\text{day}$), indicating rapid cell division during the exponential phase. In contrast, IMMA 14 showed the lowest specific growth rate on same day ($\mu = 0.15/\text{day}$), suggesting slower metabolic activity and reduced adaptability. The other isolates IMMA 11, 13, 15, and 16 demonstrated moderate growth performance.

Division time increased progressively in all microalgal species, showing an inverse relationship with the specific growth rate. This trend indicates that cells divide more slowly as time progresses, likely due to nutrient depletion or accumulation of metabolic byproducts. On day 14, IMMA 12 again displayed the shortest division time (3.32 days), reflecting its efficient and rapid cell division. while, IMMA 14 had the longest division time (4.54 days), consistent with its relatively low growth rate. IMMA 11 and IMMA 13 exhibited a steady increase in division time but performed better than IMMA 14. Meanwhile, IMMA 15 and IMMA 16 maintained relatively shorter division times than IMMA 14, indicating moderate growth efficiency. IMMA 12 emerges as the most promising strain for applications requiring rapid and sustained microalgal growth.

5.1.5. Estimation of pigments among microalgal species

Along with tocopherol, pigments such as β -carotene also show strong ROS scavenging properties due to their ability to neutralize free radicals. Therefore, we have estimated the chlorophyll a, chlorophyll b and carotenoid content among all the six microalgal species.

From our experimental data, we have found the highest total Chlorophyll, ($\sim 24.33 \mu\text{g/mL}$) in IMMA 12, followed by ($21.40 \mu\text{g/mL}$) in IMMA15, ($20.67 \mu\text{g/mL}$) in IMMA 11, ($18.84 \mu\text{g/mL}$) in IMMA 16, ($18.43 \mu\text{g/mL}$) in IMMA 13 and lowest ($16.92 \mu\text{g/mL}$) in IMMA 14 at 28th day of the stationary phase in **Figure 18**.

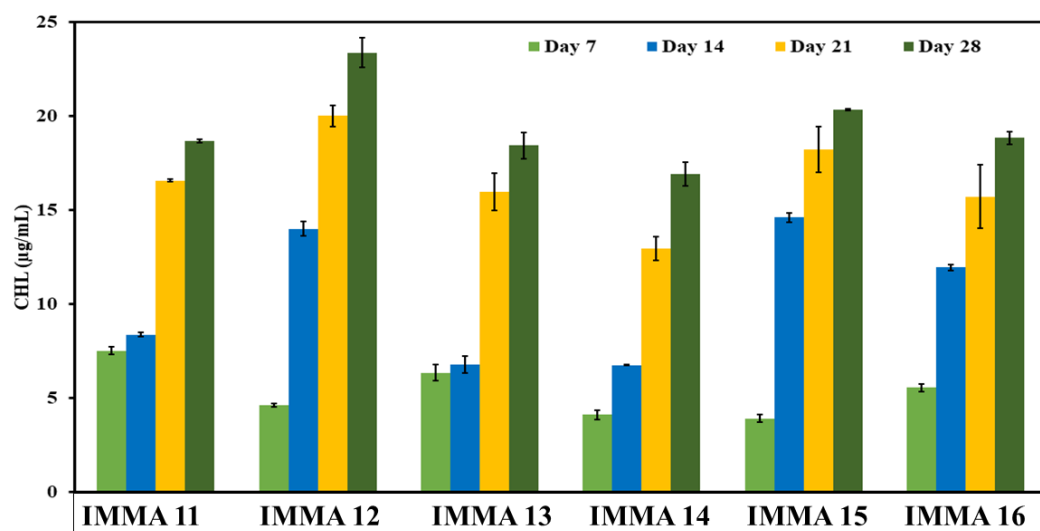


Figure 18. Graph depicting the chlorophyll profile of microalgal species at 4 different days of different growth phase

5.1.6 Tocopherol content

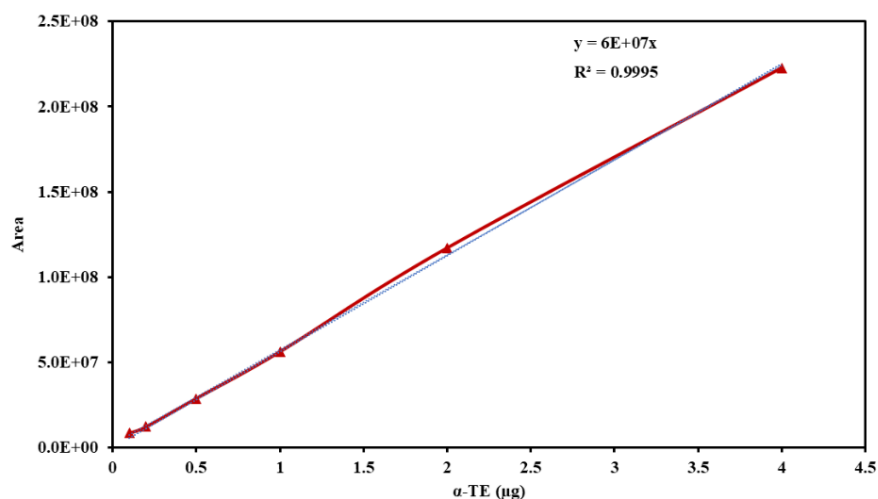


Figure 19. Tocopherol standard calibration curve

Figure 19 depicts the relationship between known concentrations of standard tocopherol and their corresponding absorbance values, allowing for the quantification of tocopherol in unknown samples based on their absorbance. The tocopherol content of all six microalgal species was analysed using high-performance liquid chromatography (HPLC) to

identify the species with the highest tocopherol production potential. A standard curve was prepared using concentrations 1 $\mu\text{g/mL}$, 10 $\mu\text{g/mL}$, 20 $\mu\text{g/mL}$, 50 $\mu\text{g/mL}$, 100 $\mu\text{g/mL}$, 150 $\mu\text{g/mL}$ and 200 $\mu\text{g/mL}$ tocopherol to ensure accurate quantification.

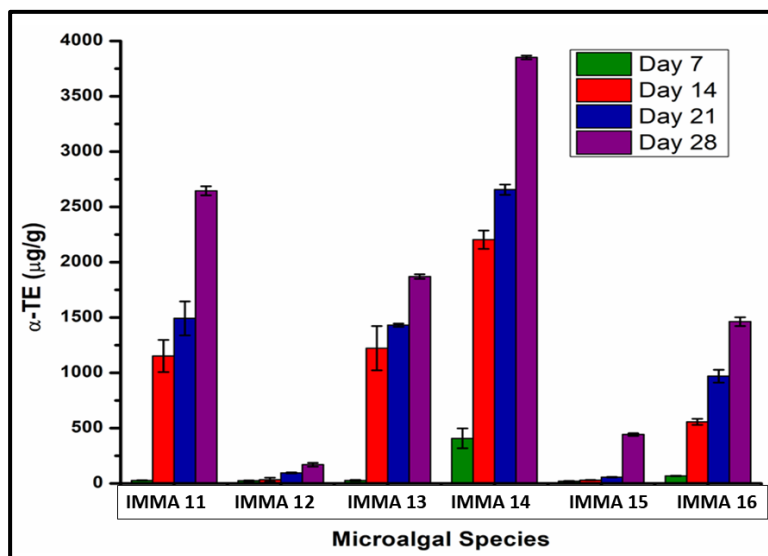
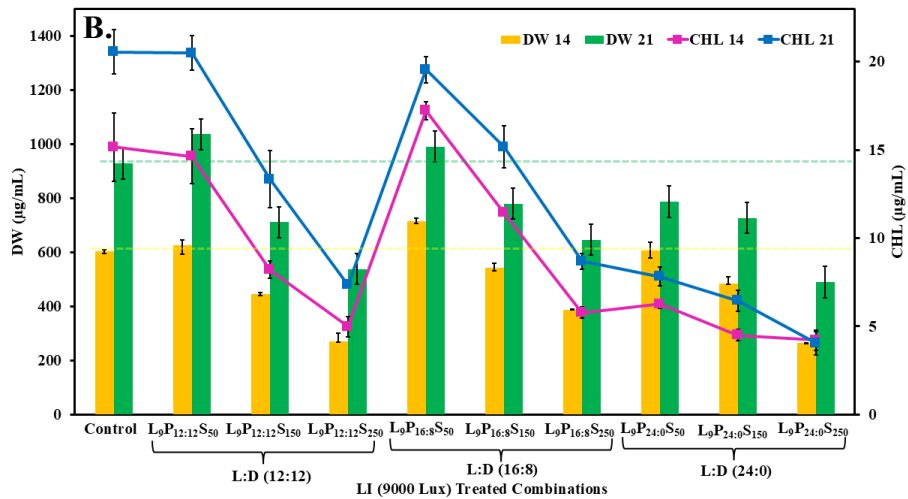
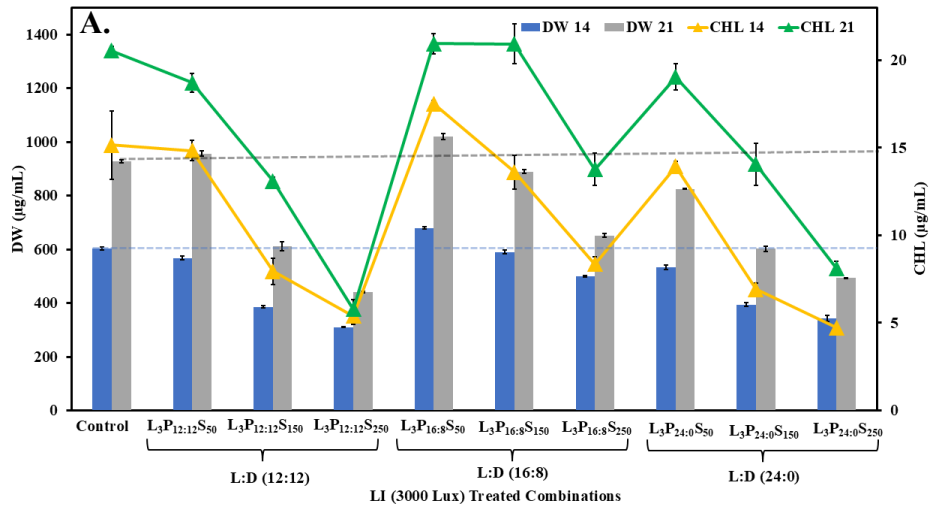


Figure 20. The graph depicts the tocopherol content in 6 native microalgal species (IMMA 11- IMMA 16) measured over 4 time points in different growth phase

In **Figure 20** IMMA 14 showing the highest tocopherol content $3851 \pm 16.47 \mu\text{g/g}$ on the day 28, making it the best performer, tocopherol content is gradually increasing over time across the all species and peaking at day 28. IMMA 12 and IMMA 15 show very low tocopherol accumulation in comparison to other species. IMMA 11, 13, 16 showing significant increases by day 28 but are still lower than IMMA 14. The trend in increasing tocopherol with depleting nutrition, increasing stress and decreasing healthy cells proving fact of literature that as stress increases production of tocopherol increases.

5.2. Experiment on selected microalgal species IMMA 12

5.2.1. Biomass and chlorophyll accumulation in IMMA 12 species under 27 different abiotic factor combinations



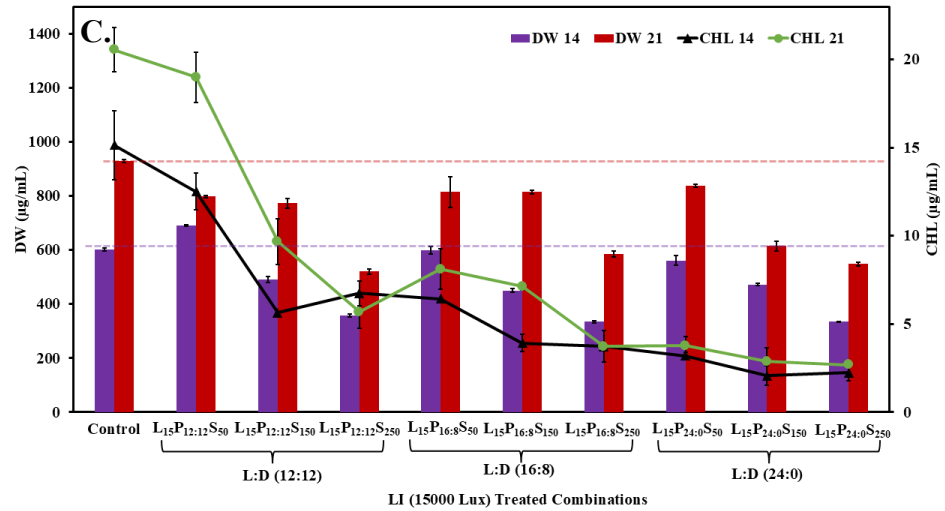


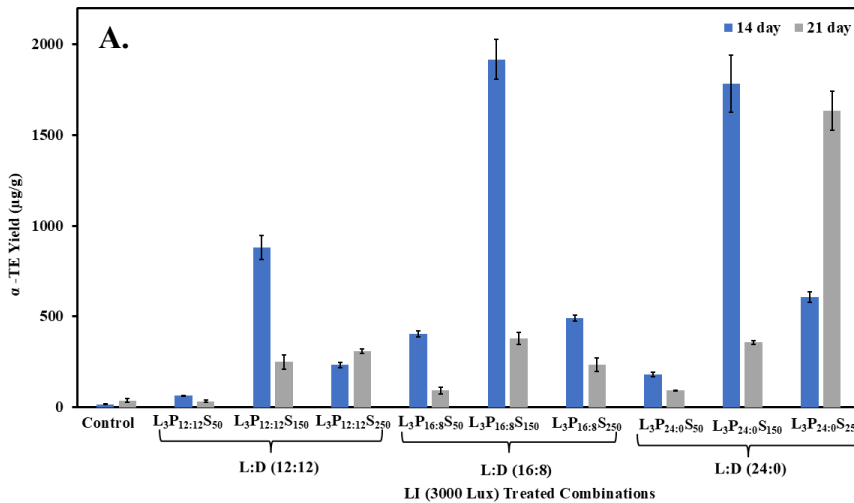
Figure 21. Biomass and chlorophyll accumulation under 27 different abiotic factor combinations (A) 3000 Lux; (B) 9000 Lux; (C) 15000 Lux

In **Figure 21.A**, where light intensity was maintained at a constant 3000 Lux, variations in photoperiod (12:12, 16:8, 24:0 hours) and salt concentration were tested. The highest biomass accumulation occurred in L₃P_{16:8}S₅₀ (679.45 µg/mL), which was 12.80 % higher than the control L₃P_{12:12}S₀ (602.37 µg/mL) on day 14. On day 21, this value increased by 9.8 % to 1019.07 µg/mL, compared to the control's 928.11 µg/mL. In **Figure 21.B**, where light intensity was set at 9000 Lux, L₉P_{16:8}S₅₀ showed the highest increase in biomass accumulation (18.70 %, 715.05 µg/mL) on day 14, while L₉P_{12:12}S₅₀ showed an 11.56 % increase (1035.47 µg/mL) on day 21, compared to the control L₃P_{12:12}S₀ (928.11 µg/mL). **Figure 21.C**, where light intensity was constant at 15000 Lux, revealed that L₁₅P_{12:12}S₅₀ had the highest biomass increase of 14.68 % (690.81 µg/mL) on day 14.

The overall highest biomass accumulation observed was 18.70 % on day 14 and 11.56 % on day 21, with other abiotic combinations showing a decrease in biomass compared to the control. A consistent trend across all three graphs showed that as salt stress increased from 50 mM to 250 mM, biomass accumulation decreased.

Similarly, the highest total chlorophyll increase (15.58 %) was observed in L₃P_{16:8}S₅₀ on day 14, while a 7 % increase was seen in L₁₅P_{12:12}S₅₀ on day 21. Very low chlorophyll accumulation was observed with the 15000 Lux combination. As with biomass, an inverse relationship was observed between salt stress and chlorophyll accumulation, where higher salt concentrations resulted in lower chlorophyll levels. The combination of 15000 Lux, a 24-hour photoperiod, and high salt stress 250 (S₂₅₀) negatively affected both biomass and chlorophyll accumulation. In general, samples from day 21 showed higher values for both dry weight and chlorophyll compared to day 14, indicating continued growth over time. Overall, the experiment suggests that a 16:8 light: dark cycle with moderate salt stress levels optimizes algal biomass and chlorophyll production over time.

5.2.2. Tocopherol yield of microalgal species IMMA 12 under 27 different abiotic factor combinations



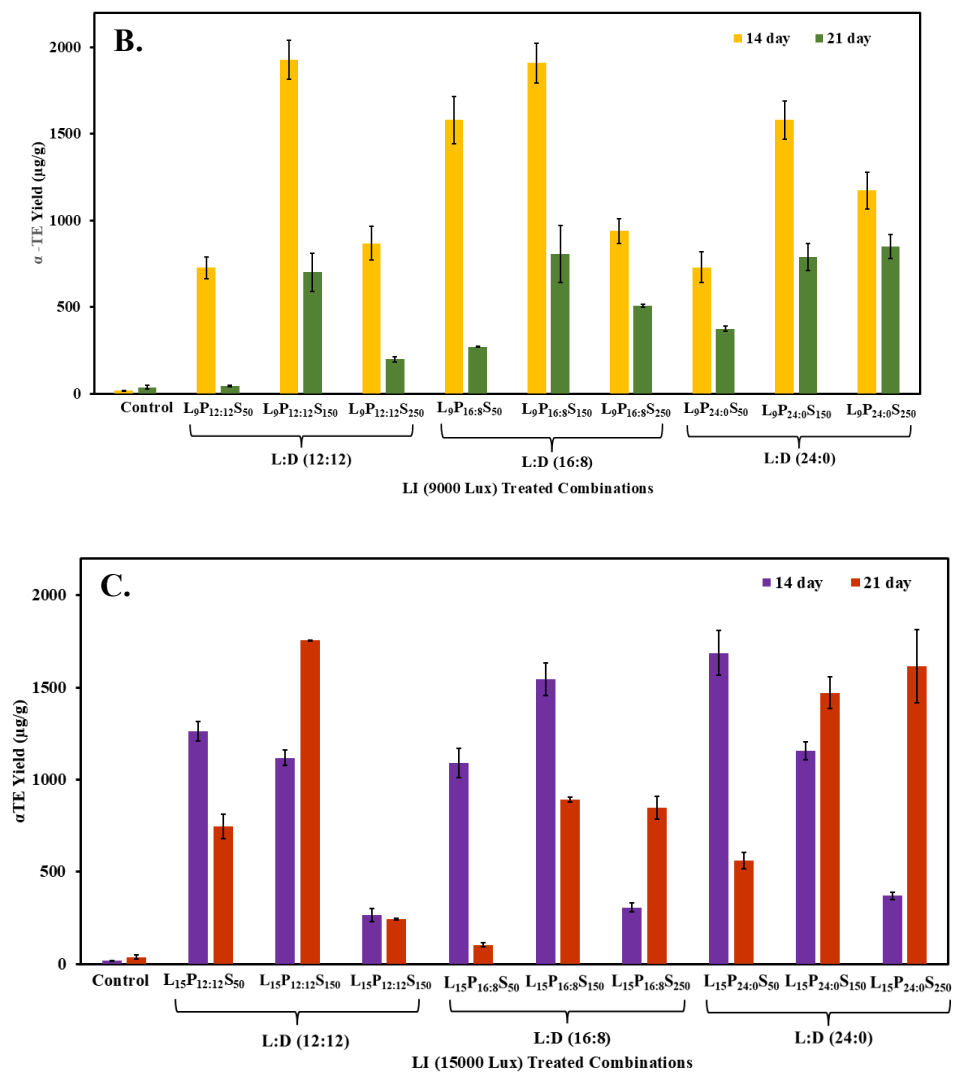


Figure 22. α -TE accumulation in IMMA 12 under 27 different abiotic factor combinations (A) 3000 Lux; (B) 9000 Lux; (C) 15000 Lux

In **Figure 22.A** where the light intensity was set at 3000 Lux, the highest α -Tocopherol yield ($1916 \pm 110 \mu\text{g/g}$) was observed at L₃P_{16:8}S₁₅₀ on day 14, followed by L₃P_{24:0}S₁₅₀ with $1782 \pm 156 \mu\text{g/g}$. In most of the combinations, α -TE were higher on day 14 than on day 21, except for L₃P_{24:0}S₂₅₀ ($1634 \pm 107 \mu\text{g/g}$), suggesting early accumulation of α -TE. The control and 12:12 photoperiods had relatively low α -TE yields. In **Figure 22.B**, where light intensity was constant at 9000 Lux, α -TE accumulation was significantly higher compared to 3000 Lux and 15000 Lux, indicating

that moderate light intensity and salinity promote higher α -TE production. Day 14 again showed the highest yield across all treatments, with L₉P_{12:12}S₁₅₀ and L₉P_{16:8}S₁₅₀ yielding $1927 \pm 113 \mu\text{g/g}$ and $1910 \pm 114 \mu\text{g/g}$, respectively. On day 21, α -TE levels generally decreased, possibly due to utilization or degradation over time. In **Figure 22.C**, L₁₅P_{12:12}S₁₅₀ exhibited the highest α -TE yield ($1756 \pm 1.36 \mu\text{g/g}$) on day 21, significantly outperforming other 12:12 combinations. Additionally, L₁₅P_{12:12}S₁₅₀ on day 14 and L₁₅P_{24:0}S₂₅₀ on day 21 showed high α -TE yields of $1686 \pm 121 \mu\text{g/g}$ and $1616 \pm 198 \mu\text{g/g}$, respectively. The production of α -TE was notably influenced by the interaction of photoperiod and salt stress, with day 14 being the optimal time for harvesting the highest α -TE yield across all light intensities. Overall, the maximum α -TE accumulation was observed in L₉P_{12:12}S₁₅₀ on day 14, which was 83.78 times higher than the control, while on day 21, L₁₅P_{12:12}S₁₅₀ yielded 47.76 times higher than the control.

5.2.3. SEM characterization of IMMA 12

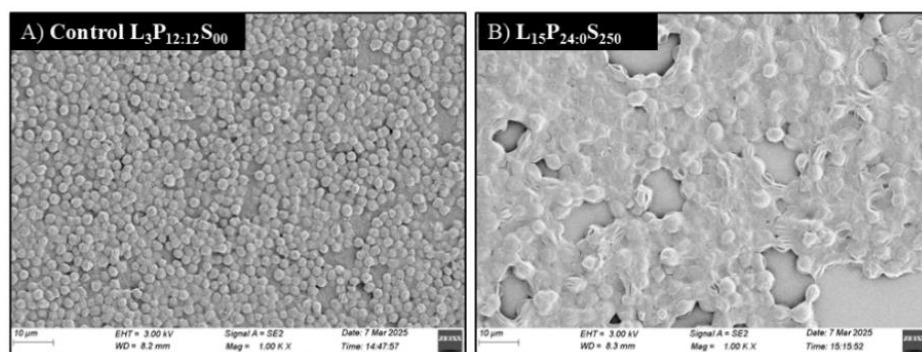


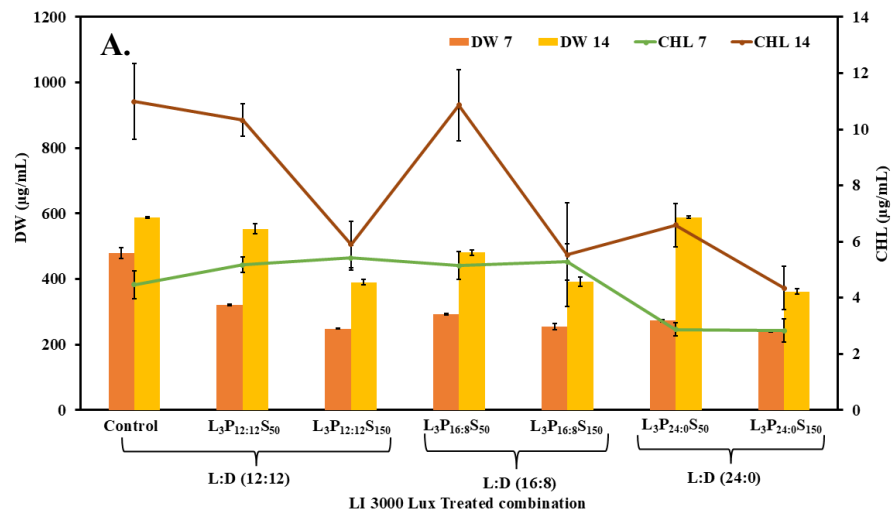
Figure 23. SEM images of IMMA 12 species of microalgae at lowest and highest abiotic factor

In **Figure 23.A**, Under control conditions, SEM images of microalgal cells show a smooth, intact, and spherical shape, with a uniform distribution, indicating that the cells are healthy, metabolically active, and not exposed to external stressors.

In contrast, under high abiotic factors **Figure 23.B**, cells in the $L_{15}P_{24}S_{250}$ treatment exhibit deformations, ruptured membranes, and irregular shapes. The cell structure appears compromised or lysed. This condition involved continuous high light exposure (24 hours) and elevated salt stress, which likely triggered both oxidative and osmotic stress, leading to the production of reactive oxygen species (ROS), potentially contributing to an increase in α -TE production.

5.3. Experiment on selected microalgal species IMMA 14

5.3.1. Biomass and chlorophyll accumulation in the IMMA 14 species under 18 different abiotic factor combinations



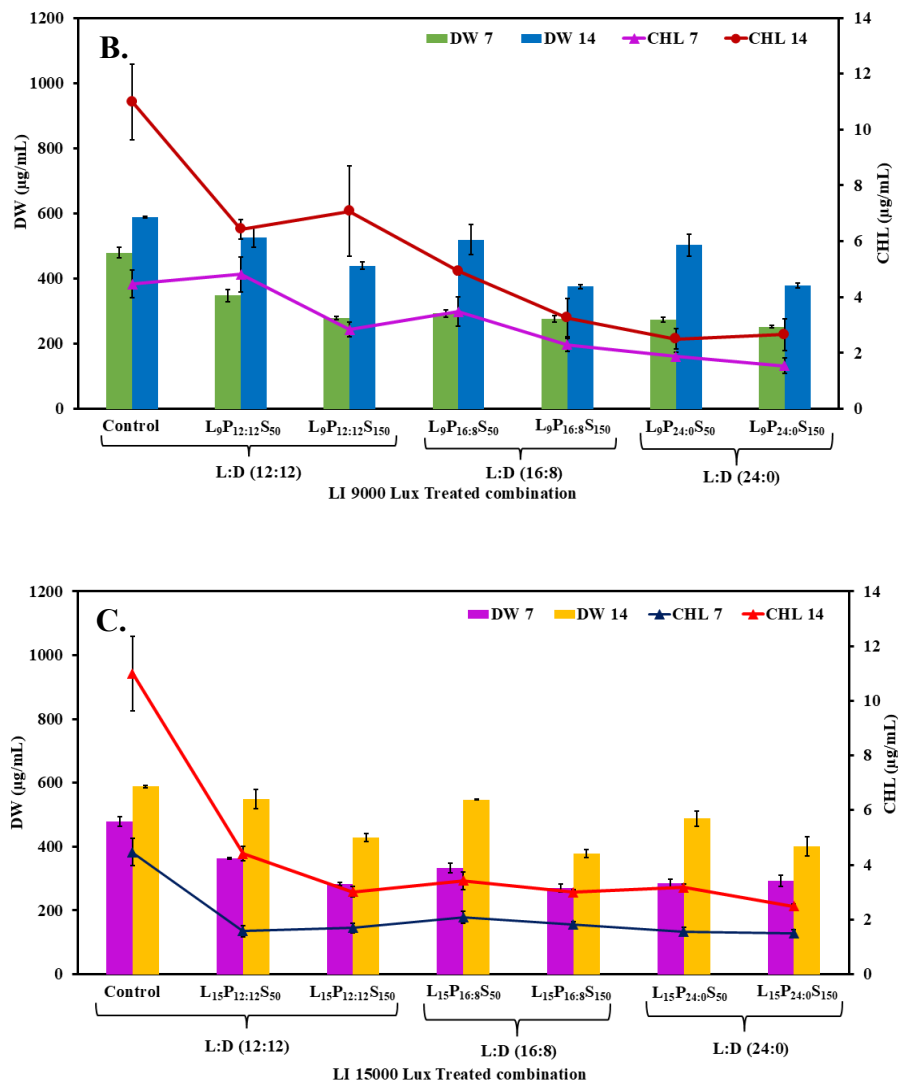
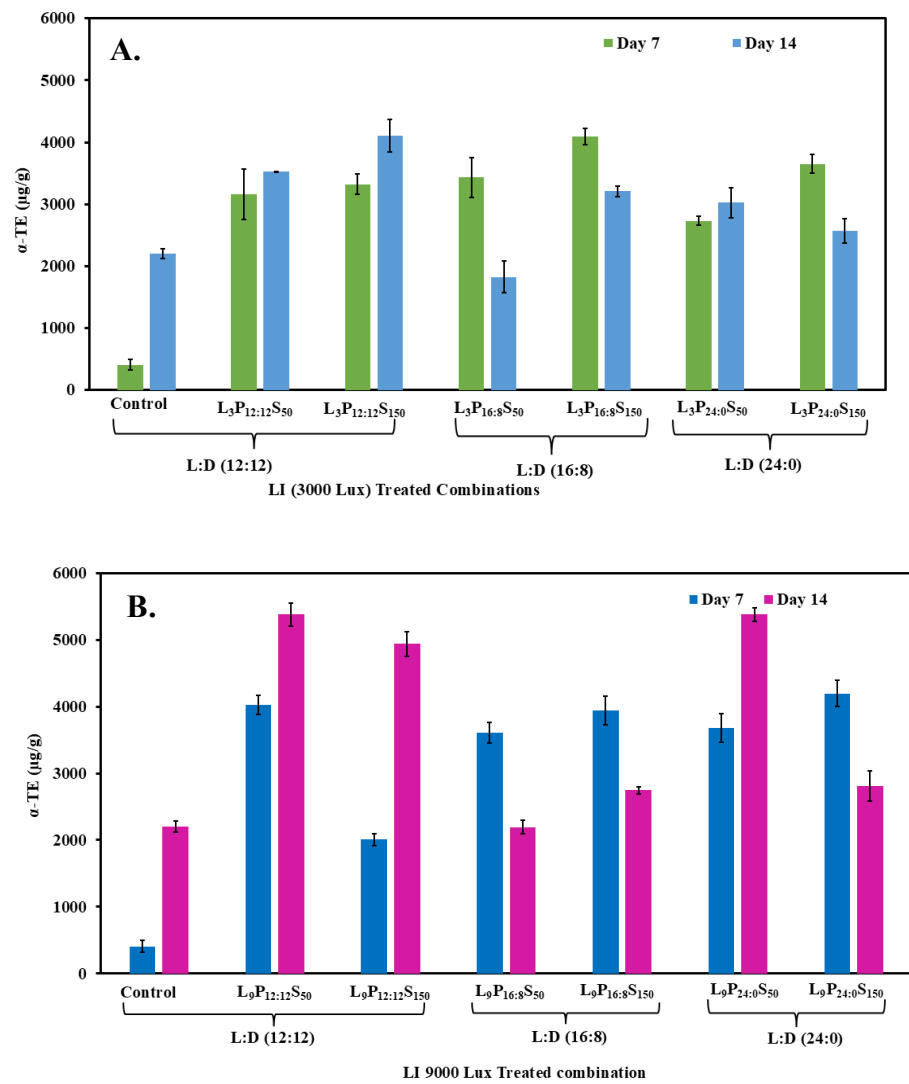


Figure 24. Biomass and chlorophyll accumulation of IMMA 14 under 18 different abiotic factor combinations (A) 3000 Lux; (B) 9000 Lux; (C) 15000 Lux

In **Figure 24.A** the 3000 Lux light intensity treatment, the highest chlorophyll (CHL) content was observed in the control ($11 \pm 1.35 \mu\text{g/g}$) and in the L₃P_{16:8}S₅₀ combination ($12.33 \pm 0.57 \mu\text{g/g}$), particularly on day 14. Both CHL and biomass increased from day 7 to day 14 across all treatments. In **Figure 24.B** the 9000 Lux light intensity treatment, biomass significantly increased by day 14 in most of the treatments; however, CHL did not show similar growth, especially in high-stress conditions like the 24:0 light/dark

cycle. In **Figure 24.C** Under the 15000 Lux treatment, CHL content sharply decreased in all treatments compared to the control. While biomass continued to increase by day 14, chlorophyll accumulation declined. Overall, both biomass and chlorophyll content were highest under low light conditions (3000 Lux), with a noticeable decrease as light intensity and salinity increased, likely due to photooxidative stress.

5.3.2. α -TE accumulation in the IMMA 14 under 18 different abiotic factor combinations



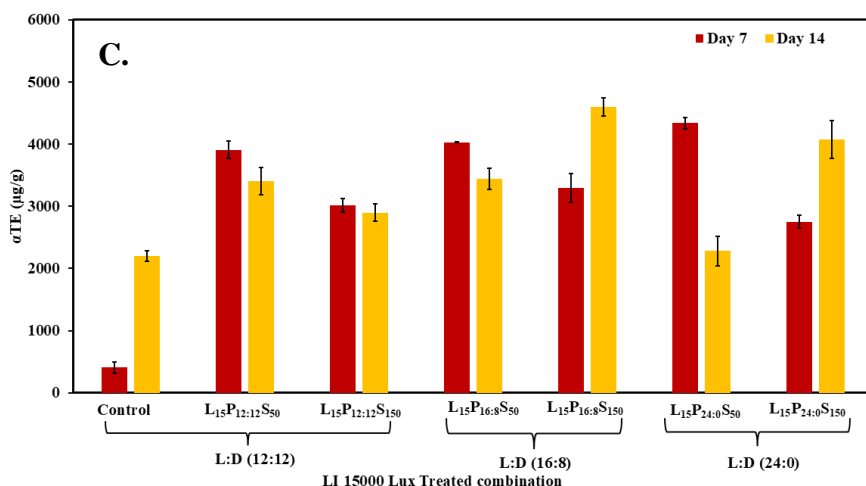


Figure 25. α -TE accumulation in IMMA 14 under 18 different abiotic factor combinations (A) 3000 Lux; (B) 9000 Lux; (C) 15000 Lux

In **Figure 25.A**, under 3000 Lux light intensity, the highest tocopherol yields were observed in the $L_3P_{12:12}S_{150}$ combination on day 14 (4109 ± 262 $\mu\text{g/g}$), followed by $L_3P_{16:8}S_{150}$ on day 7 (4093 ± 135 $\mu\text{g/g}$). On day 7, a higher salt concentration of 150 mM resulted in increased tocopherol content compared to the 50 mM concentration in the same combination. The control on day 7 showed lower tocopherol accumulation. In **Figure 25.B**, under 9000 Lux light intensity, the highest tocopherol production occurred on day 14 in $L_9P_{12:12}S_{50}$ (5378 ± 174 $\mu\text{g/g}$) and $L_9P_{24:0}S_{50}$ (5377 ± 106 $\mu\text{g/g}$). $L_9P_{16:8}S_{50}$ and $L_9P_{16:8}S_{150}$ performed less effectively in this treatment. In **Figure 25.C**, under 15000 Lux light intensity, tocopherol production decreased as salinity increased from 50 mM to 150 mM on day 7. The highest tocopherol production in this treatment was observed in $L_{15}P_{16:8}S_{150}$ (4598 ± 147 $\mu\text{g/g}$) and $L_{15}P_{24:0}S_{50}$ (4339 ± 92 $\mu\text{g/g}$) on both day 14 and day 7 respectively.

5.3.3. SEM characterization of IMMA 14

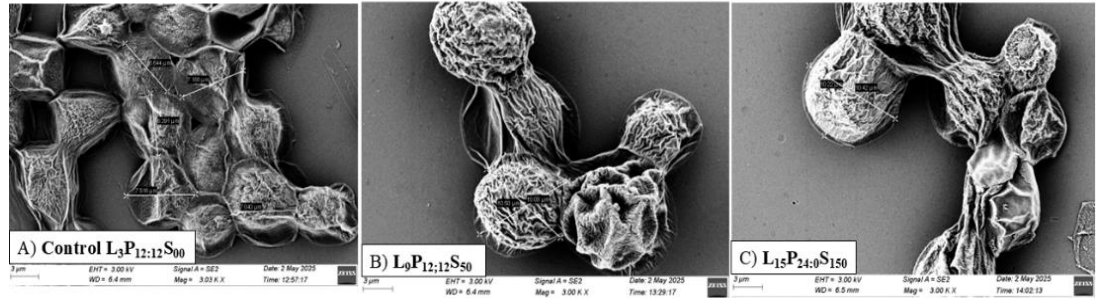


Figure 26. SEM characterization of IMMA 14 under (A) Control (L₃P₁₂S₅₀) (B) L₉P₁₂S₅₀ (C) Highest stress (L₁₅P₂₄S₁₅₀)

In **Figure 26.A**, under control conditions, SEM images showed algal cells with smooth surfaces and strong morphology, indicating healthy, metabolically active cells with intact membranes and optimal turgor pressure, suggesting no exposure to external stressors.

In **Figure 26.B**, when exposed to 50 mM NaCl under 9000 Lux light and a 12:12 light-dark cycle, subtle but noticeable changes occurred, including slight surface roughening and deformation. These alterations were likely due to osmotic imbalance as cells lost water to the hypertonic environment. This early response may also involve changes in the extracellular matrix and the flexibility of the cell wall, which are typically linked to adaptive stress mechanisms. Despite some cytoplasm shrinkage, studies indicate that biomass accumulation can still increase due to cell enlargement and the accumulation of osmoregulatory compounds (Ahmad et al., 2019; Pan et al., 2024).

In contrast, under high salinity conditions (150 mM NaCl) and continuous 15000 Lux light (24-hour photoperiod) in **Figure 26.C**, severe cellular collapse and deformation were observed. These changes signify a critical threshold beyond which the cells can no longer maintain homeostasis. The compromised integrity of the cell wall, shown by rifting and peeling, points to reduced cellular viability and impaired growth. The

formation of palmelloid structures, a survival mechanism observed in these conditions, was noted. (Farkas et al., 2023; Hernández-García & Martínez-Jerónimo, 2023) suggest that these clusters offer protection, as the mucilaginous matrix helps shield individual cells from direct salt exposure, enhancing their survival prospects.

5.4. Estimating in-vitro hydrogen peroxide scavenging activity α -tocopherol rich extract

The hydrogen peroxide scavenging activity of IMMA 14 microalgae crude extract was evaluated and compared to that of the positive control Thiamine at an equivalent concentration of 400 ng/mL. The α -tocopherol rich crude extract exhibited a notably higher scavenging capacity, with approximately 82 % inhibition of hydrogen peroxide in **Table 5** in contrast to Thiamine, which showed around 42 % activity under the same conditions. This marked difference in antioxidant effectiveness illustrates the strong capacity of IMMA 14 α -tocopherol rich extract to neutralize hydrogen peroxide, a reactive oxygen species known to contribute significantly to oxidative stress and cellular damage. The potent antioxidant action observed in the IMMA 14 α -tocopherol rich crude extract can be primarily ascribed to the presence of α -tocopherol, among other bioactive constituents. Tocopherols are known lipophilic antioxidants with the ability to neutralize reactive oxygen species. Investigations reported hydrogen peroxide scavenging activities of α -tocopherol within the range of about 37.7 % to 44.58 % at concentrations comparable to those commonly used in in-vitro antioxidant assays. For example, α -tocopherol exhibited approximately 37.7 % inhibition of hydrogen peroxide in assays comparing scavenging activity alongside compounds like trolox (Tohma & Gulçin, 2010). Other studies found α -tocopherol activity at 39.26 % to 44.58 % under similar assay conditions (Keser et al., 2012). Further, α -tocopherol demonstrated inhibition around 39.3 % in related research (Gulcin et al., 2003).

Table 5. Antioxidant activity assay of α -tocopherol rich algal extract

Extract	α - Tocopherol Conc. (mg/mL)	Antioxidant Activity (% inhibition)	Antioxidant Assay	Reference
<i>Desmodemus</i> sp.	0.36	29	DPPH	(Safafar et al., 2015)
<i>Dunaliella salina</i>	0.125	27	DPPH	
<i>Nanochloropsis limnetica</i>	0.021	35	DPPH	
<i>Nannochloropsis salina</i>	0.044	30	DPPH	
<i>Chlorella sorokiniana</i>	0.034	34	DPPH	
<i>Spirulina</i>	0.5	94	H ₂ O ₂ Scavenging assay	(Santiago-Morales et al., 2018)
IMMA 14 algal extract	0.4	82	H ₂ O ₂ Scavenging assay	Current study

Encapsulation or extraction processes that retain tocopherol in natural forms within microalgal matrices have been reported to result in potent antioxidant activities. For example, encapsulated α -tocopherol showed substantial antioxidant potential, corresponding to about 43 % radical scavenging in DPPH assays in prior research, supporting the idea that tocopherol contributes prominently to the antioxidant capacity of such extracts (Selamat et al., 2018). Importantly, natural extracts like those from IMMA 14 may contain various tocopherol isoforms (α -, β -, γ -, δ -) and tocotrienols, collectively amplifying the antioxidative effect beyond that of isolated α -tocopherol (Ohkatsu et al., 2001). Furthermore, the observed high scavenging activity of the IMMA 14 extract against hydrogen peroxide underscores its capability in mitigating oxidative stress, a critical factor involved in the pathogenesis of numerous chronic diseases. Hydrogen peroxide, while less reactive than other oxygen radicals, can diffuse through membranes and generate more harmful radicals via Fenton-type reactions, contributing to cellular dysfunction (Coulombier et al., 2021). Therefore, an antioxidant source that efficiently scavenges hydrogen peroxide holds therapeutic and nutraceutical promise.

Chapter 6

Conclusions and future perspectives

6.1. Conclusions

- This study involved an in-depth analysis of the morphology and biochemical properties of six native microalgal isolates (IMMA 11 to 16), all classified under the Chlorophyceae class of the Chlorophyta division. Although all the species were green, photosynthetic, and unicellular, they differed in cell size. Among them, IMMA 12 (1.2–1.8 μm) and IMMA 15 (1.8–2.2 μm) were the smallest, while the others—IMMA 11, 13, 14, and 16—had larger cells, measuring between 5 and 10 μm .
- Growth assessment using $\text{OD}_{680 \text{ nm}}$ readings revealed clear distinctions in growth patterns among the isolates. IMMA 12 exhibited the most rapid growth, followed by IMMA 15, whereas IMMA 14 showed the slowest progression. Maximum biomass accumulation for all species occurred on the 28th day, with IMMA 11 reaching the highest concentration at $1760 \pm 80 \mu\text{g/mL}$. A decline in specific growth rates over time suggested a reduction in available nutrients. Initially, IMMA 12 had the highest growth rate, while IMMA 14 recorded the lowest. This trend was mirrored in cell division times, where IMMA 12 had the shortest division interval in log phase, and IMMA 14 the longest.
- Pigment analysis revealed that IMMA 12 contained the highest concentration of chlorophyll ($\sim 24.33 \mu\text{g/mL}$), with IMMA 15 and IMMA 11 following closely behind. In contrast, IMMA 14 produced the least chlorophyll. Tocopherol levels, measured using HPLC, were found to be highest in IMMA 14, reaching $3851 \pm 16.47 \mu\text{g/g}$ on day 28. Across all isolates, tocopherol

content increased progressively over time, peaking on the 28th day, particularly under nutrient-limited and stress-inducing conditions.

- Abiotic stress experiments involved varying light intensities (3000, 9000, 15000 Lux), photoperiods (12:12, 16:8, 24:0), and salt concentrations (50, 150, 250 mM). The optimal combination for biomass and chlorophyll accumulation was 9000 Lux, 16:8 light cycle, and 50 mM salt, showing up to 18.7 % increase in biomass. As salt increased to 250 mM, growth and pigment content declined, especially under 15000 Lux and 24 h light. Chlorophyll and biomass generally increased between days 14–21, but stress beyond moderate levels was detrimental.
- Tocopherol production was significantly affected by combined stress conditions. Under an intensity of 9000 Lux, the maximum α -tocopherol yield was recorded at 5378 ± 174 $\mu\text{g/g}$ (in treatment L₉P_{12:12}S₅₀ on day 14), marking a 2.44-fold increase compared to the control. Most treatments showed day 14 as the most favorable time for tocopherol extraction. Field emission scanning electron microscopy (FE-SEM) images under control conditions revealed intact, smooth cell surfaces. However, when exposed to intense stress (15000 Lux light, continuous 24-hour illumination, and 250 mM salt concentration), cells showed deformation and membrane damage, signs of oxidative and osmotic stress. This correlated with a rise in tocopherol levels, highlighting its role in cellular defense as an antioxidant.
- The antioxidant potential of the IMMA 14 extract, which contains a high concentration of α -tocopherol, was assessed using hydrogen peroxide scavenging assays. The extract showed 82 % inhibition, substantially higher than the 42 % observed for thiamine. Previous studies report that tocopherol's radical scavenging activity typically ranges between 37 % and 45 %,

emphasizing the superior effectiveness of the IMMA 14 extract. This strong antioxidant performance indicates its promise for use in nutraceutical formulations, likely due to the presence of various tocopherol isoforms and other complementary bioactive constituents.

6.2. Future perspectives

The findings of this study highlight the potential of native Chlorophyceae strains, especially IMMA 14, for further development in both scientific and practical fields. Future research should explore upscaling these microalgae under carefully controlled abiotic conditions to enhance the production of valuable compounds like tocopherols and pigments. Investigating the genetic and molecular mechanisms behind their stress responses could help identify important pathways that regulate antioxidant synthesis. This knowledge may also support targeted improvements through strain selection or modification. Additionally, examining the full range of bioactive substances in these algae could reveal new compounds with health-promoting properties. There is also potential to assess their use in systems like bioreactors or integrated with wastewater treatment, combining biomass production with environmental benefits. Advancing this work into real-world applications will require collaboration across fields such as microbiology, process engineering, and product development.

References

1. Admins. (2024, May 14). OXIDATIVE STRESS AND INFLAMMATION IN CARDIOVASCULAR DISEASES. *SVEIKATOS MOKSLAI / HEALTH SCIENCES*. <https://sm-hs.eu/oxidative-stress-and-inflammation-in-cardiovascular-diseases/>
2. Aghdassi, E., Wendland, B. E., Steinhart, A. H., Wolman, S. L., Jeejeebhoy, K., & Allard, J. P. (2003). Antioxidant vitamin supplementation in Crohn's disease decreases oxidative stress: A randomized controlled trial. *The American Journal of Gastroenterology*, 98(2), 348–353. <https://doi.org/10.1111/j.1572-0241.2003.07226.x>
3. Ahmad, S., Kothari, R., Shankarayan, R., & Tyagi, V. V. (2019). Temperature dependent morphological changes on algal growth and cell surface with dairy industry wastewater: An experimental investigation. *3 Biotech*, 10(1), 24. <https://doi.org/10.1007/s13205-019-2008-x>
4. Aksoz, E., Korkut, O., Aksit, D., & Gokbulut, C. (2020). Vitamin E (α -, β + γ - and δ -tocopherol) levels in plant oils. *Flavour and Fragrance Journal*, 35(5), 504–510. <https://doi.org/10.1002/ffj.3585>
5. Andonova, L., Georgieva, M., & Zlatkov, A. (n.d.). FREE RADICALS, OXIDATIVE STRESS, AND DISEASES ASSOCIATED WITH THEM. *Oxidative Stress*, 62(2).
6. Ayala, A., Muñoz, M. F., & Argüelles, S. (2014). Lipid Peroxidation: Production, Metabolism, and Signaling Mechanisms of Malondialdehyde and 4-Hydroxy-2-Nonenal. *Oxidative Medicine and Cellular Longevity*, 2014(1), 360438. <https://doi.org/10.1155/2014/360438>
7. Baboo, K. D., Chen, Z.-Y., & Zhang, X.-M. (2019). Role of Oxidative Stress and Antioxidant Therapies in Endometriosis. *Reproductive and Developmental Medicine*, 3(3), 170. <https://doi.org/10.4103/2096-2924.268154>
8. Bewick, M., Coutie, W., & Tudhope, G. R. (1987). Superoxide dismutase, glutathione peroxidase and catalase in the red cells of

patients with malignant lymphoma. *British Journal of Haematology*, 65(3), 347–350. <https://doi.org/10.1111/j.1365-2141.1987.tb06866.x>

9. Bhatti, J. S., Sehrawat, A., Mishra, J., Sidhu, I. S., Navik, U., Khullar, N., Kumar, S., Bhatti, G. K., & Reddy, P. H. (2022). Oxidative stress in the pathophysiology of type 2 diabetes and related complications: Current therapeutics strategies and future perspectives. *Free Radical Biology and Medicine*, 184, 114–134. <https://doi.org/10.1016/j.freeradbiomed.2022.03.019>
10. Borowitzka, M. A. (1992). Algal biotechnology products and processes—Matching science and economics. *Journal of Applied Phycology*, 4(3), 267–279. Scopus. <https://doi.org/10.1007/BF02161212>
11. Boukhenouna, S., Wilson, M. A., Bahmed, K., & Kosmider, B. (2018). Reactive Oxygen Species in Chronic Obstructive Pulmonary Disease. *Oxidative Medicine and Cellular Longevity*, 2018(1), 5730395. <https://doi.org/10.1155/2018/5730395>
12. Bouyahya, A., Bakrim, S., Chamkhi, I., Taha, D., El Omari, N., El Mneyiy, N., El Hachlafi, N., El-Shazly, M., Khalid, A., Abdalla, A. N., Goh, K. W., Ming, L. C., Goh, B. H., & Aanniz, T. (2024). Bioactive substances of cyanobacteria and microalgae: Sources, metabolism, and anticancer mechanism insights. *Biomedicine & Pharmacotherapy = Biomedecine & Pharmacotherapie*, 170, 115989. <https://doi.org/10.1016/j.biopha.2023.115989>
13. Carballo-Cárdenas, E. C., Tuan, P. M., Janssen, M., & Wijffels, R. H. (2003). Vitamin E (α -tocopherol) production by the marine microalgae *Dunaliella tertiolecta* and *Tetraselmis suecica* in batch cultivation. *Biomolecular Engineering*, 20(4), 139–147. [https://doi.org/10.1016/S1389-0344\(03\)00040-6](https://doi.org/10.1016/S1389-0344(03)00040-6)
14. Casetta, I., Govoni, V., & Granieri, E. (2005). Oxidative stress, antioxidants and neurodegenerative diseases. *Current Pharmaceutical Design*, 11(16), 2033–2052. <https://doi.org/10.2174/1381612054065729>
15. Coulombier, N., Jauffrais, T., & Lebouvier, N. (2021). Antioxidant Compounds from Microalgae: A Review. *Marine Drugs*, 19(10), Article 10. <https://doi.org/10.3390/md19100549>

16. David, B., Wolfender, J.-L., & Dias, D. A. (2015). The pharmaceutical industry and natural products: Historical status and new trends. *Phytochemistry Reviews*, 14(2), 299–315. <https://doi.org/10.1007/s11101-014-9367-z>
17. Dobrek, Ł. (2022). Oxidative stress mechanisms as potential therapeutic targets in chronic kidney disease. *Medical Studies*, 38(2), 163–170. <https://doi.org/10.5114/ms.2022.117714>
18. Durmaz, Y. (2007). Vitamin E (α -tocopherol) production by the marine microalgae *Nannochloropsis oculata* (Eustigmatophyceae) in nitrogen limitation. *Aquaculture*, 272(1), 717–722. <https://doi.org/10.1016/j.aquaculture.2007.07.213>
19. Durmaz, Y., Donato, M., Monterio, M., Gouveia, L., Nunes, M. L., Gama Pereira, T., Gokpinar, S., & Bandarra, N. M. (2008). *Effect of Temperature on Growth and Biochemical Composition (Sterols, α -tocopherol, Carotenoids, Fatty Acid Profiles) of the Microalga, Isochrysis galbana*. <http://hdl.handle.net/10524/19257>
20. Engin, K. N. (2009). Alpha-tocopherol: Looking beyond an antioxidant. *Molecular Vision*, 15, 855–860.
21. Ercal, N., Gurer-Orhan, H., & Aykin-Burns, N. (2001). Toxic Metals and Oxidative Stress Part I: Mechanisms Involved in Metal-induced Oxidative Damage. *Current Topics in Medicinal Chemistry*, 1(6), 529–539. <https://doi.org/10.2174/1568026013394831>
22. Farkas, A., Pap, B., Zsíros, O., Patai, R., Shetty, P., Garab, G., Bíró, T., Ördög, V., & Maróti, G. (2023). Salinity stress provokes diverse physiological responses of eukaryotic unicellular microalgae. *Algal Research*, 73, 103155. <https://doi.org/10.1016/j.algal.2023.103155>
23. Forman, H. J., & Zhang, H. (2021). Targeting oxidative stress in disease: Promise and limitations of antioxidant therapy. *Nature Reviews Drug Discovery*, 20(9), 689–709. <https://doi.org/10.1038/s41573-021-00233-1>
24. Gambhir, L., Tyagi, G., Bhardwaj, R., Kapoor, N., & Sharma, G. (2022). *Perturbation of Cellular Redox Status: Role of Nrf2, a Master Regulator of Cellular Redox*. 28. <https://doi.org/10.5772/intechopen.102319>

25. Gelain, D. P., Antonio Behr, G., Birnfeld De Oliveira, R., & Trujillo, M. (2012). Antioxidant Therapies for Neurodegenerative Diseases: Mechanisms, Current Trends, and Perspectives. *Oxidative Medicine and Cellular Longevity*, 2012, 1–2. <https://doi.org/10.1155/2012/895153>
26. Gershenzon, J., & Dudareva, N. (2007). The function of terpene natural products in the natural world. *Nature Chemical Biology*, 3(7), 408–414. <https://doi.org/10.1038/nchembio.2007.5>
27. Ghosh, T., Chouhan, V., Ojha, K., Bala, K., & Bux, F. (2025). Effects of antibiotic supplementation vs. Nutrient stress on α -linolenic acid and α -tocopherol in *Scenedesmus* sp. *Bioresource Technology*, 418, 131968. <https://doi.org/10.1016/j.biortech.2024.131968>
28. Grujicic, J., & Allen, A. R. (2024). MnSOD Mimetics in Therapy: Exploring Their Role in Combating Oxidative Stress-Related Diseases. *Antioxidants*, 13(12), 1444. <https://doi.org/10.3390/antiox13121444>
29. Guillard, R. R. L., Kilham, P., & Jackson, T. A. (1973). Kinetics of Silicon-Limited Growth in the Marine Diatom *Thalassiosira pseudonana* Hasle and Heimdal (=cyclo^{TEL}la Nana Hustedt). *Journal of Phycology*, 9(3), 233–237. <https://doi.org/10.1111/j.1529-8817.1973.tb04086.x>
30. Gulcin, İ., Buyukokuroglu, M. E., & Kufrevioglu, O. I. (2003). Metal chelating and hydrogen peroxide scavenging effects of melatonin. *Journal of Pineal Research*, 34(4), 278–281. <https://doi.org/10.1034/j.1600-079X.2003.00042.x>
31. Gupta, S., Sekhon, L., Kim, Y., & Agarwal, A. (2010). The Role of Oxidative Stress and Antioxidants in Assisted Reproduction. *Current Women's Health Reviews*, 6(3), 227–238. <https://doi.org/10.2174/157340410792007046>
32. Hardoko, H., Febriani, A., & Siratantri, T. (2015). Invitro Antidiabetic Activities of Agar, Agarosa, and Agarpectin from *Gracilaria gigas* Seaweed. *Jurnal Pengolahan Hasil Perikanan Indonesia*, 18(2), Article 2. <https://doi.org/10.17844/jphpi.v18i2.10608>

33. Hernández-García, C. I., & Martínez-Jerónimo, F. (2023). Changes in the morphology and cell ultrastructure of a microalgal community exposed to a commercial glyphosate formulation and a toxigenic cyanobacterium. *Frontiers in Microbiology*, 14. <https://doi.org/10.3389/fmicb.2023.1195776>
34. Irato, P., & Santovito, G. (2021). Enzymatic and Non-Enzymatic Molecules with Antioxidant Function. *Antioxidants*, 10(4), Article 4. <https://doi.org/10.3390/antiox10040579>
35. Jamdade, C. B., & Bodare, R. D. (n.d.). A MINI REVIEW ON FREE RADICALS-GENERATED IN BIOLOGICAL SYSTEM. *World Journal of Pharmaceutical Research*, 12(3).
36. Jiang, Q. (2014). Natural forms of vitamin E: Metabolism, antioxidant and anti-inflammatory activities and the role in disease prevention and therapy. *Free Radical Biology & Medicine*, 72, 76–90. <https://doi.org/10.1016/j.freeradbiomed.2014.03.035>
37. Jones, D. P., & Radi, R. (2014). Redox Pioneer: Professor Helmut Sies. *Antioxidants & Redox Signaling*, 21(18), 2459–2468. <https://doi.org/10.1089/ars.2014.6037>
38. Kamal-Eldin, A., & Appelqvist, L.-Å. (1996). The chemistry and antioxidant properties of tocopherols and tocotrienols. *Lipids*, 31(7), 671–701. <https://doi.org/10.1007/BF02522884>
39. Katoch, N., Kaur, P., Kashyap, P., Gupta, S., & Dahiya, R. (2013). *Role of Oxidative Stress in Cardiovascular Diseases*. <https://www.semanticscholar.org/paper/Role-of-Oxidative-Stress-in-Cardiovascular-Diseases-Katoch-Kaur/55b99d31b5798f8bc5d504e33cdc0870e5cd73e9>
40. Keser, S., Celik, S., Turkoglu, S., Yilmaz, O., & Turkoglu, I. (2012). Hydrogen peroxide radical scavenging and total antioxidant activity of hawthorn. *Chem J*, 2(1), 9–12.
41. Kumagai, S., Jikimoto, T., & Saegusa, J. (2003). [Pathological roles of oxidative stress in autoimmune diseases]. *Rinsho Byori. The Japanese Journal of Clinical Pathology*, 51(2), 126–132.
42. Lichtenthaler, H. K. (1987). [34] Chlorophylls and carotenoids: Pigments of photosynthetic biomembranes. In *Methods in*

Enzymology (Vol. 148, pp. 350–382). Academic Press.
[https://doi.org/10.1016/0076-6879\(87\)48036-1](https://doi.org/10.1016/0076-6879(87)48036-1)

43. Ljubic, A., Holdt, S. L., Jakobsen, J., Bysted, A., & Jacobsen, C. (2021). Fatty acids, carotenoids, and tocopherols from microalgae: Targeting the accumulation by manipulating the light during growth. *Journal of Applied Phycology*, 33(5), 2783–2793.
<https://doi.org/10.1007/s10811-021-02503-2>
44. Lushchak, V. I., & Semchuk, N. M. (2012). Tocopherol biosynthesis: Chemistry, regulation and effects of environmental factors. *Acta Physiologiae Plantarum*, 34(5), 1607–1628.
<https://doi.org/10.1007/s11738-012-0988-9>
45. Martins, A., Vieira, H., Gaspar, H., & Santos, S. (2014). Marketed Marine Natural Products in the Pharmaceutical and Cosmeceutical Industries: Tips for Success. *Marine Drugs*, 12(2), Article 2.
<https://doi.org/10.3390/md12021066>
46. Menzel, M., Ramu, S., Calvén, J., Olejnicka, B., Sverrild, A., Porsbjerg, C., Tufvesson, E., Bjermer, L., Akbarshahi, H., & Uller, L. (2019). Oxidative Stress Attenuates TLR3 Responsiveness and Impairs Anti-viral Mechanisms in Bronchial Epithelial Cells From COPD and Asthma Patients. *Frontiers in Immunology*, 10.
<https://doi.org/10.3389/fimmu.2019.02765>
47. Meulmeester, F. L., Luo, J., Martens, L. G., Mills, K., van Heemst, D., & Noordam, R. (2022). Antioxidant Supplementation in Oxidative Stress-Related Diseases: What Have We Learned from Studies on Alpha-Tocopherol? *Antioxidants*, 11(12), Article 12.
<https://doi.org/10.3390/antiox11122322>
48. Modaresi, A., Nafar, M., & Sahraei, Z. (2015). Oxidative stress in chronic kidney disease. *Iranian Journal of Kidney Diseases*, 9(3), 165–179.
49. Mokrosnop, V. M., Polishchuk, A. V., & Zolotareva, E. K. (2016). Accumulation of α -tocopherol and β -carotene in *Euglena gracilis* Cells Under Autotrophic and Mixotrophic Culture Conditions. *Applied Biochemistry and Microbiology*, 52(2), 216–221.
<https://doi.org/10.1134/S0003683816020101>

50. Mudimu, O., Koopmann, I. K., Rybalka, N., Friedl, T., Schulz, R., & Bilger, W. (2017). Screening of microalgae and cyanobacteria strains for α -tocopherol content at different growth phases and the influence of nitrate reduction on α -tocopherol production. *Journal of Applied Phycology*, 29(6), 2867–2875. <https://doi.org/10.1007/s10811-017-1188-1>
51. Munné-Bosch, S. (2005). The role of α -tocopherol in plant stress tolerance. *Journal of Plant Physiology*, 162(7), 743–748. <https://doi.org/10.1016/j.jplph.2005.04.022>
52. Nabavi, S., Ebrahimzadeh, M., Fazelian, M., & Eslami, B. (2009). In vitro Antioxidant and Free Radical Scavenging Activity of Diospyros lotus and Pyrus boissieriana growing in Iran. *Pharmacognosy Magazine*, 5(18), 122–126.
53. Naito, Y., & Yoshikawa, T. (2011). *Neutrophil-Dependent Oxidative Stress in Inflammatory Gastrointestinal Diseases* (Y. Naito, M. Suematsu, & T. Yoshikawa, Eds.; Vol. 29, pp. 35–54). S. Karger AG. <https://doi.org/10.1159/000319940>
54. Ohkatsu, Y., Kajiyama, T., & Arai, Y. (2001). Antioxidant activities of tocopherols. *Polymer Degradation and Stability*, 72(2), 303–311. [https://doi.org/10.1016/S0141-3910\(01\)00022-2](https://doi.org/10.1016/S0141-3910(01)00022-2)
55. Onaca, M., Onaca, A., Erdei, A., Popa, A. R., & Georgios, P. (2010). PARAMETERS OF OXIDATIVE STRESS IN PATIENTS WITH DIABETES. *Romanian Journal of Diabetes Nutrition and Metabolic Diseases*, 17(3), Article 3.
56. Ördög, V., Stirk, W. A., Bálint, P., van Staden, J., & Lovász, C. (2012). Changes in lipid, protein and pigment concentrations in nitrogen-stressed Chlorella minutissima cultures. *Journal of Applied Phycology*, 24(4), 907–914. <https://doi.org/10.1007/s10811-011-9711-2>
57. Pan, Y., Amenorfenyo, D. K., Dong, M., Zhang, N., Huang, X., Li, C., & Li, F. (2024). Effects of salinity on the growth, physiological and biochemical components of microalga Euchlorocystis marina. *Frontiers in Marine Science*, 11. <https://doi.org/10.3389/fmars.2024.1402071>

58. Pancha, I., Chokshi, K., George, B., Ghosh, T., Paliwal, C., Maurya, R., & Mishra, S. (2014). Nitrogen stress triggered biochemical and morphological changes in the microalgae *Scenedesmus* sp. CCNM 1077. *Bioresource Technology*, 156, 146–154. <https://doi.org/10.1016/j.biortech.2014.01.025>
59. Pham-Huy, L. A., He, H., & Pham-Huy, C. (2008). Free Radicals, Antioxidants in Disease and Health. *International Journal of Biomedical Science : IJBS*, 4(2), 89–96.
60. Pizzino, G., Irrera, N., Cucinotta, M., Pallio, G., Mannino, F., Arcoraci, V., Squadrito, F., Altavilla, D., & Bitto, A. (2017). Oxidative Stress: Harms and Benefits for Human Health. *Oxidative Medicine and Cellular Longevity*, 2017, 8416763. <https://doi.org/10.1155/2017/8416763>
61. Pradhan, B., Nayak, R., Patra, S., Jit, B. P., Ragusa, A., & Jena, M. (2021). Bioactive Metabolites from Marine Algae as Potent Pharmacophores against Oxidative Stress-Associated Human Diseases: A Comprehensive Review. *Molecules*, 26(1), Article 1. <https://doi.org/10.3390/molecules26010037>
62. Reddy, V. P. (2023). Oxidative Stress in Health and Disease. *Biomedicines*, 11(11), Article 11. <https://doi.org/10.3390/biomedicines11112925>
63. Ryter, S. W., Kim, H. P., Hoetzel, A., Park, J. W., Nakahira, K., Wang, X., & Choi, A. M. K. (2007). Mechanisms of Cell Death in Oxidative Stress. *Antioxidants & Redox Signaling*, 9(1), 49–89. <https://doi.org/10.1089/ars.2007.9.49>
64. Saldeen, K., & Saldeen, T. (2005). Importance of tocopherols beyond α -tocopherol: Evidence from animal and human studies. *Nutrition Research*, 25(10), 877–889. <https://doi.org/10.1016/j.nutres.2005.09.019>
65. Sastre-Oliva, T., Corbacho-Alonso, N., Albo-Escalona, D., Lopez, J. A., Lopez-Almodovar, L. F., Vázquez, J., Padial, L. R., Mourino-Alvarez, L., & Barderas, M. G. (2022). The Influence of Coronary Artery Disease in the Development of Aortic Stenosis and the Importance of the Albumin Redox State. *Antioxidants*, 11(2), Article 2. <https://doi.org/10.3390/antiox11020317>

66. Sawhney, S. K. (n.d.). *Oxidative stress, Mitochondrial dysfunction and Neuro- degenerative diseases: A Review*.
67. Silva Ortíz, Y. L., de Sousa, T. C., Krukalis, N. E., Galeano García, P., Brango-Vanegas, J., Soller Ramada, M. H., & Franco, O. L. (2025). The Role of Amphibian AMPs Against Oxidative Stress and Related Diseases. *Antibiotics*, 14(2), Article 2. <https://doi.org/10.3390/antibiotics14020126>
68. Singh, R., Paliwal, C., Nesamma, A. A., Narula, A., & Jutur, P. P. (2020). Nutrient Deprivation Mobilizes the Production of Unique Tocopherols as a Stress-Promoting Response in a New Indigenous Isolate *Monoraphidium* sp. *Frontiers in Marine Science*, 7. <https://doi.org/10.3389/fmars.2020.575817>
69. Soengas, P., Rodríguez, V. M., Velasco, P., & Cartea, M. E. (2018). Effect of Temperature Stress on Antioxidant Defenses in Brassica oleracea. *ACS Omega*, 3(5), 5237–5243. <https://doi.org/10.1021/acsomega.8b00242>
70. T, V., Bansal, N., Kumari, K., Prashat G, R., Sreevathsa, R., Krishnan, V., Kumari, S., Dahuja, A., Lal, S. K., Sachdev, A., & Praveen, S. (2017). Comparative Analysis of Tocopherol Biosynthesis Genes and Its Transcriptional Regulation in Soybean Seeds. *Journal of Agricultural and Food Chemistry*, 65(50), 11054–11064. <https://doi.org/10.1021/acs.jafc.7b03448>
71. Thoré, E. S. J., Muylaert, K., Bertram, M. G., & Brodin, T. (2023). Microalgae. *Current Biology*, 33(3), R91–R95. <https://doi.org/10.1016/j.cub.2022.12.032>
72. Tohma, H. S., & Gulçin, I. (2010). Antioxidant and Radical Scavenging Activity of Aerial Parts and Roots of Turkish Liquorice (*Glycyrrhiza Glabra* L.). *International Journal of Food Properties*, 13(4), 657–671. <https://doi.org/10.1080/10942911003773916>
73. Udaypal, Goswami, R. K., Mehariya, S., & Verma, P. (2024). Microalgae-derived tocopherols: Biotechnological advances in production and its therapeutic potentials. *Sustainable Chemistry and Pharmacy*, 42, 101791. <https://doi.org/10.1016/j.scp.2024.101791>
74. Voronkova, Y. S., Voronkova, O. S., Gorban, V. A., & Holoborodko, K. K. (2018). Oxidative stress, reactive oxygen

species, antioxidants: A review. *Ecology and Noospherology*, 29(1), 52–55. <https://doi.org/10.15421/031809>

75. Vranová, E., Coman, D., & Gruissem, W. (2013). Network Analysis of the MVA and MEP Pathways for Isoprenoid Synthesis. *Annual Review of Plant Biology*, 64(Volume 64, 2013), 665–700. <https://doi.org/10.1146/annurev-arplant-050312-120116>
76. Wang, Y., Fu, X., & Li, H. (2025). Mechanisms of oxidative stress-induced sperm dysfunction. *Frontiers in Endocrinology*, 16, 1520835. <https://doi.org/10.3389/fendo.2025.1520835>
77. Wróblewski, M., Wróblewska, W., & Sobiesiak, M. (2024). The Role of Selected Elements in Oxidative Stress Protection: Key to Healthy Fertility and Reproduction. *International Journal of Molecular Sciences*, 25(17), 9409. <https://doi.org/10.3390/ijms25179409>
78. Yamasaki, H., Itoh, R. D., Mizumoto, K. B., Yoshida, Y. S., Otaki, J. M., & Cohen, M. F. (2025). Spatiotemporal Characteristics Determining the Multifaceted Nature of Reactive Oxygen, Nitrogen, and Sulfur Species in Relation to Proton Homeostasis. *Antioxidants & Redox Signaling*, 42(7–9), 421–441. <https://doi.org/10.1089/ars.2023.0544>
79. Yoshida, Y., Niki, E., & Noguchi, N. (2003). Comparative study on the action of tocopherols and tocotrienols as antioxidant: Chemical and physical effects. *Chemistry and Physics of Lipids*, 123(1), 63–75. [https://doi.org/10.1016/S0009-3084\(02\)00164-0](https://doi.org/10.1016/S0009-3084(02)00164-0)
80. Zhan, H., Yu, G., Zheng, M., Zhu, Y., Ni, H., Oda, T., & Jiang, Z. (2022). Inhibitory effects of a low-molecular-weight sulfated fucose-containing saccharide on α -amylase and α -glucosidase prepared from ascophyllan. *Food & Function*, 13(3), 1119–1132. <https://doi.org/10.1039/D1FO03331J>